

EXTRACTION OF ACCELERATION SIGNALS RELATED TO
MOTOR UNIT ACTION POTENTIALS

By
CHRISTOPHER ORSI, B.ENG.

A Thesis
Submitted to the School of Graduate Studies
in Partial Fulfillment of the Requirements
for the Degree
Master of Engineering

McMaster University

© Copyright by Christopher Orsi, July 2000

MASTER OF ENGINEERING (2000)
(Electrical Engineering)

McMASTER UNIVERSITY
Hamilton, Ontario

TITLE: Extraction of Acceleration Signals Related to Motor Unit Action Potentials

AUTHOR: Christopher Orsi, B.Eng. (Queen's University)

SUPERVISOR: Dr. H. de Bruin

NUMBER OF PAGES: xi, 110

ABSTRACT

A novel method is described for recording the electrical and contractile properties of a number of human motor units using surface electromyography (EMG) and accelerometry. The motor units are recruited by stimulating the median nerve at the wrist using surface electrodes and graded stimulus amplitudes. The resulting M-waves and acceleration signals are decomposed into individual motor unit action potentials and acceleration responses using a pattern recognition technique.

Results obtained for the left and right thenar muscles of three healthy male subjects are presented. For the six thenars, a minimum of 9 and maximum of 17 MUs could be studied, resulting in a total sample of 72 MUs. Using data from these subjects, a study of the relative efficacy of various EMG pattern recognition strategies including those based on time, Fourier and wavelet analysis is also analyzed.

The findings of the present study agree well with similar research using force measurement. It may be concluded that acceleration measurement can be used as an alternative to isometric twitch forces and may be more suitable because of the relative ease of instrumentation and lack of subject discomfort. It also follows that a pattern recognition scheme based on MUAPs allows the measurement of contractile properties of many more MUs for each muscle studied than can be accomplished by other published techniques.

ACKNOWLEDGMENTS

I would like to thank Dr. H. deBruin for his advice, enthusiasm and support during the development of this thesis. He has helped make my experience at McMaster an enlightening and rewarding one. Many thanks go out to Dr. A.J. McComas, Dr. V. Galea, Dr. R. Szlavik, Nafia Al-Mutawaly and Cheryl Gies for their encouragement and help. Special recognition should also be given to the Biomedical Engineering Staff at Chedoke-McMaster Hospital for their assistance and camaraderie. A large thank you goes out to my friends and family for their endless support. And finally, I want to thank my parents, who prepared me so well to meet the challenges encountered.

TABLE OF CONTENTS

LIST OF FIGURES.....	ix
LIST OF TABLES.....	x
LIST OF ABBREVIATIONS.....	xi
1. INTRODUCTION	
1.1 Introduction.....	1
1.2 Summary of Chapters.....	2
2. BACKGROUND	
2.1 The Motor Unit.....	4
2.2 Disorders of the Motor Unit.....	8
2.3 The McComas Technique.....	10
2.4 Assumptions of the McComas Technique.....	12
2.5 Improvements to the McComas Technique.....	13
2.6 Measurement of the Contractile Properties of Motor Units.....	15
2.7 Conclusion.....	19
3. MEASUREMENT AND ANALYSIS SYSTEM	
3.1 Introduction.....	20
3.1.1 Subject Setup.....	20
3.1.2 Electrodes.....	23
3.1.3 Accelerometers.....	23
3.1.4 EMG Amplifier.....	25
3.1.5 Acceleration Amplifiers.....	25

3.1.6	Stimulator.....	26
3.1.7	Data Acquisition Board.....	27
3.1.8	Personal Computer.....	28
3.2	Software.....	28
3.2.1	System Parameters and Initialization.....	30
3.2.2	Acquire.....	30
3.2.3	Read From File.....	34
3.2.4	Signal Processing.....	35
3.2.4.1	EMG 60-Hz Noise.....	35
3.2.4.2	EMG Stimulus Artifact and Baseline Detrending....	38
3.2.4.3	Acceleration Noise Sources.....	39
3.2.4.4	Acceleration Filtering and Composite Response.....	40
3.2.4.5	Unacceptable Responses and Averaging.....	41
3.2.4.6	Signal Feature Extraction.....	42
3.2.4.7	Fourier and Wavelet Transforms.....	42
3.2.5	Recording Session Protocol.....	43
3.2.5.1	Instrumentation.....	44
3.2.5.2	MEP Acquisition.....	44
3.2.5.3	Sub-Threshold Acquisition.....	45
3.2.6	Response Collection.....	46
3.2.7	Response Classification.....	47
3.2.8	Session Termination.....	49

3.2.9	Response Storage.....	50
4. EMG AND ACCELERATION SIGNALS		
4.1	Thenar Studies.....	53
4.2	All-or-Nothing Response of M-Waves.....	53
4.3	Alternation.....	54
4.4	EMG Responses.....	58
4.5	Acceleration Responses.....	60
4.5.1	Smallest MU AR and Averaging.....	62
4.5.2	Force and Acceleration.....	62
4.5.3	Potentialiation.....	63
4.6	Electrical Properties.....	64
4.6.1	MUAP Peak to Peak and Area.....	65
4.6.2	MUAP Latency.....	67
4.7	Contractile Properties.....	67
4.7.1	Peak Acceleration Magnitude and Direction.....	69
4.7.2	Peak Acceleration Latency.....	72
4.8	Relationships Between Parameters.....	75
4.9	Motor Unit Number Estimation.....	77
4.9.1	MUAP Extrapolation.....	78
4.9.2	MU Peak Acceleration / Force Extrapolation.....	81
4.9.3	Implications.....	81

5. EMG PATTERN RECOGNITION TECHNIQUES	
5.1 EMG Pattern Recognition.....	85
5.1.1 Latency Shifting.....	86
5.2 Frequency Domain Classification.....	87
5.3 Short-Time Fourier Analysis.....	90
5.4 Wavelet Based Classification.....	91
5.5 Manual Pattern Recognition.....	97
5.6 Feature Comparisons.....	98
5.7 Online vs Offline M-Wave Pattern Recognition.....	100
6. CONCLUSIONS	
6.1 Summary.....	103
6.2 Future Work.....	105
REFERENCES.....	107

LIST OF FIGURES

2.1	Structure of a Typical Motor Unit.....	5
3.1	Experimental Instrumentation.....	21
3.2	Hardware Overview.....	22
3.3	Graphical User Interface.....	29
3.4	Software Flowchart.....	31
3.5	Response Classification Flowchart.....	32
3.6	Signal Epochs.....	33
3.7	EMG Signal Processing.....	36
3.8	Smallest 6 of 14 M-Wave Templates.....	51
4.1	Alternation.....	55
4.2	Representative Extracted MUAPs.....	61
4.3	Distribution of Thenar MUAP Sizes.....	65
4.4	Distribution of Thenar MUAP Peak Latencies.....	68
4.5	Peak MU Acceleration Vectors.....	70
4.6	Distribution of Thenar MU Peak Acceleration Responses.....	71
4.7	Distribution of Thenar MU Peak Acceleration Latency.....	73
4.8	Peak to Peak Amplitude vs Peak Acceleration for Templates and Graded Responses.....	83
5.1	Daubechies 'db5' Wavelet Function and Filter Representation.....	92
5.2	Wavelet Decomposition.....	95

LIST OF TABLES

4.1	EMG and Acceleration Responses.....	59
4.2	Electrical Properties of Motor Units.....	64
4.3	Contractile Properties of Motor Units.....	67
4.4	Correlation Coefficients Between Parameters.....	76
4.5	MUNEs by M-Wave and Peak Acceleration Extrapolation.....	79
4.6	Summary of Thenar MUNEs from Recent Studies.....	80
5.1	Classification Feature Comparison by Intra-Group Standard Deviation.....	99
5.2	Classification Feature Comparison by Maximum Intra-Group Deviation...	99

LIST OF ABBREVIATIONS

AP = Action Potential

AR = Acceleration Response

CR = Composite Response (M-Wave Potentials)

EPLA = Evoked Peak Limb Acceleration

EMG = Electromyography

GUI = Graphical User Interface

MEP = Maximum Evoked Potential

MN = Motor Neuron

MU = Motor Unit

MUAP = Motor Unit Action Potential

MUAR = Motor Unit Acceleration Response

CHAPTER 1 INTRODUCTION

1.1 Introduction

A motor unit (MU), the smallest functional unit of contraction in a skeletal muscle, consists of a motor neuron (MN) and all the muscle fibers innervated by it. Excitation of the MU produces both an electrical and contractile response. In the study of normal muscle function and neuromuscular disease, the most accessible information derives from the electromyographic (EMG) signal. However, mechanical muscle properties especially at the single motor unit level are much more difficult to measure. Such information is important not only when studying normal muscle structure and function but also in diagnosing neuromuscular diseases such as those of metabolic origin where contractile properties and resistance to fatigue are important.

Electrical and contractile properties of motor units of the thenar muscle group have been studied in the past using strain gauge force transducers and careful positioning and restraints of the forearm and hand. These studies depended on intraneural or surface stimulation of single motor axons in the median nerve. To obtain the results for even a small population of motor units was necessarily very time-consuming and fatiguing to the subject.

This thesis presents a novel method for obtaining these properties for a sample of typically 10 to 20 motor units using a single recording sequence. Further, there is no requirement for rigidly restraining the limb. The present study uses noninvasive surface

EMG and accelerometry to measure and decompose electrical and acceleration responses into the contributions of individual MUs. Typical results for the left and right thenars of three healthy male volunteers are presented. Motor unit number estimates are calculated using both the electrical and contractile properties of the MU populations. The findings are related to those of other researchers measuring the electrical and contractile properties of individual thenar motor units in the past.

In an attempt to improve on previously developed M-wave decomposition techniques, an examination of the relative efficacy of various EMG pattern recognition strategies is also carried out, using data from the six thenar studies. Such strategies using time, Fourier and wavelet analysis take advantage of the ever-increasing signal processing and computing power available to EMG researchers.

1.2 Summary of Chapters

The next chapter describes the concept of the MU, some of its properties and some of the ways in which its electrical and contractile properties can be measured. Chapter 3 describes the hardware and software employed and developed for this thesis. Results of a study of six human thenars are presented in Chapter 4 and the electrical and contractile properties of the putative MUs are compared with the findings of other researchers. A discussion of the problem of alternation and the detection scheme used to alleviate it is also found in Chapter 4, along with an example and discussion of motor unit number estimation (MUNE) using both the electrical and contractile properties of the MU sample. Chapter 5 examines the relative efficacy of various EMG signal processing

techniques and pattern recognition strategies, including those based on time, Fourier and wavelet analysis. The results of a study using data from the six thenars examined in this thesis are presented. Finally, Chapter 6 concludes by summarizing the work to date and suggests topics for further investigation.

CHAPTER 2 BACKGROUND

2.1 The Motor Unit

Although a detailed description of the electrophysiological and electrochemical processes in human skeletal muscle is beyond the scope of this thesis, a brief overview follows. A more detailed description can be found in references such as Guyton and Hall (1996).

The motor unit (MU) is the smallest functional unit of contraction in human skeletal muscle. The MU size, which is a reference to the number and type of muscle fibers innervated by that unit, determines the magnitude of muscular contraction. Differences in contractile speed and fatiguability of muscular contraction are also determined by the properties of active MUs. Figure 2.1 summarizes the structure of a typical motor unit. The motor neuron (MN) cell body is located in the spinal column, and a motor axon branches off the cell body. The motor axon is protected by a myelin sheath, which also has the effect of greatly increasing the velocity of electrical transmission along the axon. The axon has terminal branches, which in turn innervate muscle fibers. A single MN may innervate a range of a few to several hundred muscle fibers depending on the muscle. The number of MUs within a particular muscle varies over a similar range.

The contraction of the muscle fibers of a MU is triggered by an electro-chemical event called the action potential (AP). In healthy nerve and muscle the AP is an all-or-

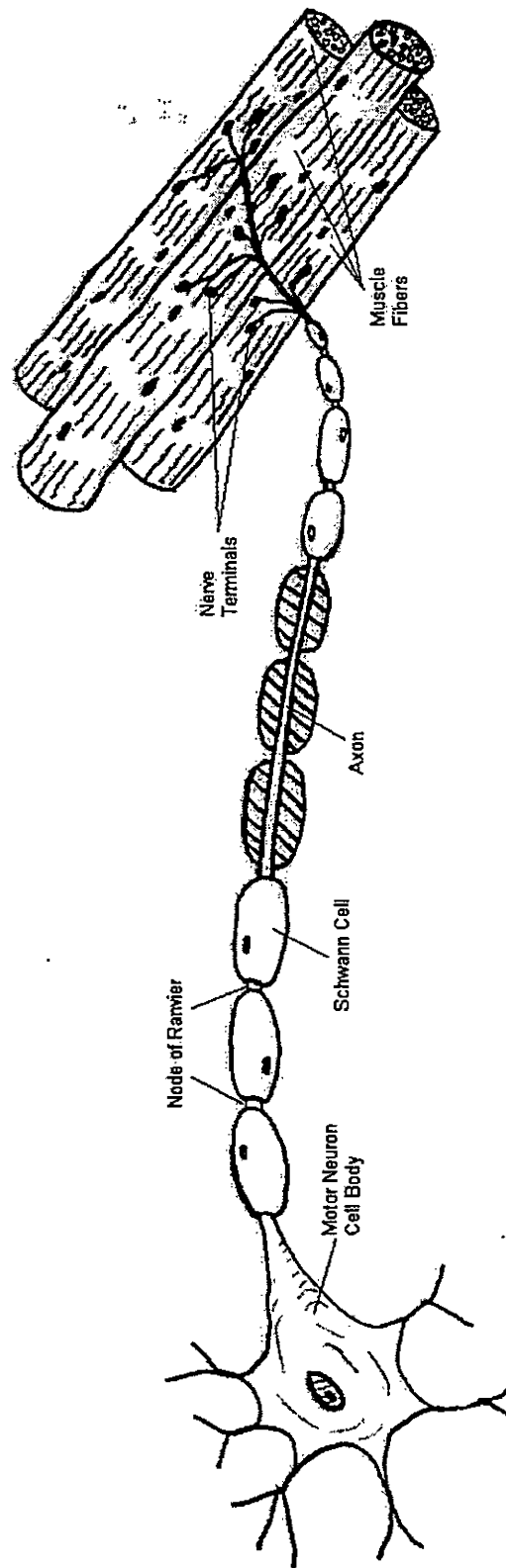


Figure 2.1. Structure of a Typical Motor Unit

nothing event. Once initiated, the AP will propagate down the axon, across the synaptic gaps at the terminal branches, and activate all the muscle fibers innervated by the MN. The AP occurs in the form of a rapid depolarization and then repolarization of the cellular membrane, which appears as a moving dipole to stationary recording electrodes.

The motor axon is demyelinated just before it enters the muscle. This area is called the end plate zone. The spatial dispersion of the terminal branches of the MN over the end plate zone results in a temporal dispersion of the individual muscle fiber APs that sum to form the motor unit action potential (MUAP). The shape of any particular MUAP will be a function of the dispersion of MN terminal branches, the number and arrangement of muscle fibers in the MU, the spatial relationship of the muscle fibers with respect to the recording electrodes, and the filtering properties of the tissues and instrumentation. Once the recording electrodes are applied and held in place, however, the all-or-nothing nature of the AP makes the shape of any particular MUAP relatively stable over time. It is this constancy of MUAP shape and size over the course of a recording session that makes MU pattern recognition possible.

When the AP reaches and travels down the innervated muscle fibers, it initiates the contractile mechanism. The force produced by the excited muscle fibers pulls on the connective tissue of the muscle, transmitting force to the muscle tendons. The tendons in turn transmit force to their associated origins and insertions on the bone. Since all MUs in a muscle transmit force through common tendons, it is reasonable to assume the force summation of two or more MUs is linear. If at least one of the tendons is attached to a limb that is free to move, the force of the MU contraction will cause the limb to

accelerate, resulting in a twitch lasting from 80 to 150 ms. Once peak twitch force has occurred, the limb returns to its resting position because of the elastic properties of tissue and gravitational or other muscle forces, undergoing a negative acceleration phase in the process. The magnitude and rate of limb movement depend on muscular contraction force, muscle fiber contractile rate, limb properties and joint dynamics.

The tension of the whole muscle is moderated by a combination of two mechanisms: increasing or decreasing the number of MUs recruited, and altering the frequency of excitation of the MUs to modulate the tension produced by the individual MUs. The strength of the MU contraction can be increased by evoking a series of twitches at a rate (typically more than 8 Hz) such that successive contractions begin before the previous ones are complete, resulting in a summation effect.

Motor unit populations in several species have commonly been subdivided into slow twitch (S), fast twitch-fatigue resistant (FR), fast twitch-fatigue intermediate (FI) and fast twitch-fatigable (FF) units on the basis of 'sag' of unfused tetani, contractile speed and fatiguability. However, the distribution of unit force seems to be continuous over a 10- to 100-fold range (e.g. Rafuse and Gordon, 1996). Nonetheless, on average, motor unit force increases in the order of $S < FR < FI = FF$ (Rafuse et al., 1997).

The number of MUs normally found in a muscle is related to the control refinement required of the muscle. The innervation ratio of the average MU, that is, the number of muscle fibers per MN, is related to the force required of the muscle. Thus the platysma, a small muscle controlling the position of the jaw, has many (approximately 1000) MUs and relatively few (an average of 27) innervated muscle fibers per MU,

whereas a large calf muscle, the medial head of the gastrocnemius, may have only 580 MUs but with approximately 70 times as many fibers per MN (Feinstein, 1955).

Because MU force has been found to increase with electrophysiological parameters of MN size such as peak to peak amplitude or area of MUAP, Henneman and colleagues suggested that: (1) the smallest axons supply fewer muscle fibers than the larger axons, i.e. the number of muscle fibers per MN (innervation ratio) is directly related to MN size; and (2) the relationship between innervation ratio and MN size accounts for the observed correlation between MU force and MN size (Henneman and Mendell, 1981).

Muscle fibers also demonstrate differences in size and histochemistry, and are commonly subdivided into type I (slow), type II (fast) fibers. The wide range of motor unit force has generally been attributed to the differences in cross-sectional area of the type I and II fibers which comprise the S, FR, FI and FF motor units as well as force per fiber area (specific force) differences between slow and fast fibers. It is possible that the relative contributions of the three factors (innervation ratio, fiber area, and specific force) to motor unit force may be related to overall muscle size and/or architecture (Rafuse et al., 1997).

2.2 Disorders of the Motor Unit

Should some of the MUs in a muscle become inoperative or impaired, two qualities of motor control can be reduced: the maximum muscle tension may be reduced and the gradation in force may become less refined. Where the primary defect in the MU

is in the MN (a neuropathy), the number of viable MUs will be reduced. This can be contrasted with the case where the primary defect is in the muscle fibers (a myopathy) and the number of useful fibers per MU is reduced.

The neuromuscular system possesses a high degree of plasticity, enabling healthy muscle fibers, which have lost their MNs, to become re-innervated by the remaining healthy MNs. The effect is that the number of MUs can be decreased while the number of operative muscle fibers, and therefore the maximal muscle tension, remains constant. In this case, while maximal muscle tension remains intact, the gradation in force will likely become less refined due to the reduced MU population. The number of viable MUs has therefore been widely used as evidence for distinguishing neuropathies from myopathies.


The concept of the MU has become important in the study and assessment of normal neuromuscular function and disorders of the neuromuscular system. A technique, such as the one presented in this thesis, of estimating the number of functional MUs and examining the electrical and contractile properties of a large sample of MUs from a given subject has tremendous importance in the field of neuromuscular physiology. As a research tool, such a technique may be used to examine several questions pertaining to neuromuscular function. In a clinical setting it may be used as a diagnostic tool, providing a means to quantify the effects of a disorder or treatment upon MUs over time.

2.3 The McComas Technique

If a pair of electrodes are applied to the skin over a nerve bundle that runs near the surface, the application of an electrical pulse across them can induce an AP in some or all of the axons within the nerve. The set of MNs that are activated will depend on the intensity and spatial distribution of the stimulus current and the activation thresholds of the individual MN axons. APs will travel down the activated axons to the muscle fibers they innervate and evoke MUAPs, which summate and can be recorded by surface electrodes placed over the muscle belly.

Briefly, the McComas technique consists of gradually increasing the stimulus amplitude under manual control while displaying the evoked responses on a storage oscilloscope to obtain a composite response (CR), which is composed of a number of discrete gradations or increments, as shown in Figure 3.8 (A). Each successive increment in this CR is assumed to be the contribution of an additional MU that has been excited.

The original intent of the McComas technique was to provide a method of calculating a motor unit number estimate (MUNE) for a given subject. By dividing the amplitude of the largest response in the CR by the number of increments, the operator obtains an estimate of the average MUAP amplitude contribution for that muscle. The operator then reduces the amplifier/oscilloscope gain and increases the stimulus amplitude until the response displays no discernable increase in amplitude. This maximum evoked potential (MEP) response comprises the summated MUAPs for all the MUs in the muscle. By dividing the amplitude of the MEP by the average MUAP amplitude, one obtains an estimate of the number of MUs in the muscle:



$$MUNE = \frac{MEP \text{ amplitude}}{\text{Average MUAP amplitude}}$$

The amplitude feature may be peak to peak, area, or in a similar fashion using contractile properties, peak force or acceleration may be substituted.

In order to use this technique, the muscle under investigation must be accessible for surface stimulation of the innervating MNs and recording of the resulting MUAPs at the muscle belly using surface electrodes. Some of the muscles that are commonly tested are the thenar, hypothenar, extensor digitorum brevis, soleus, first dorsal interosseus, and deltoid. The thenar was chosen for the present study, since it is easily accessible by the criteria outlined above and a significant research base exists concerning the electrical and contractile properties of human thenar MUs. Figure 3.1 shows the positioning of the stimulating and recording electrodes for the present study.

As shown in Figure 3.6, a typical thenar EMG response consists of a stimulus artifact caused by the volume conduction of the stimulating pulse, a propagation delay (settling time) as the AP travels down the axons and across the synaptic gaps, and the response of the summated MUAPs referred to as the M-wave (response window). Although the stimulating pulse is rectangular, the filtering properties of the tissues and electrodes result in an exponentially decaying artifact. By varying the stimulus pulse amplitude, the number of MUs in the muscle that are activated can be varied from none to all. Unfortunately, as will be explained later, there is not a one to one relationship between stimulus amplitude and the number of MUs activated.

2.4 Assumptions of the McComas Technique

As described by Doherty and Brown (1993), fundamental assumptions underlying the original manual method of McComas and colleagues (1971) and subsequent modifications including the system presented in this thesis, include:

- 1) The ability of a finely graded electrical stimulus percutaneously delivered to a motor nerve to excite, in an all-or-nothing manner, a single motor axon, and the ability to record the corresponding all-or-nothing surface-recorded motor unit action potential from the muscle.
- 2) The thresholds of at least the first few motor axons excited above threshold are sufficiently separate that graded increases in the stimulus intensity will excite, in an orderly and reproducible manner, successively higher threshold motor axons; recruitment of which will be signaled by successive quantal increases in the size of the compound M-wave through the addition of the corresponding MUAPs to the compound potential.
- 3) The first MUs excited above threshold are representative of the relative numbers of MUs of differing sizes and physiological properties normally or pathologically present in the muscle studied.

The validity of these assumptions as applied to the present study will be examined throughout the thesis. Most criticisms against the McComas technique focus on the assumption that every increment in the CR truly represents the activity of a single MU. If the stimulation thresholds of several MUs are fairly close together, upon repeated

stimulation, they may fire in various combinations to produce more CR increments than there are MUs active. This phenomenon has been referred to as alternation (McComas et al., 1971) or probabilistic activation and will be discussed in greater detail in Chapter 4.

2.5 Improvements to the McComas Technique

Ballantyne and Hansen (1974; 1975) suggested using the absolute area under the response curve as the feature upon which the MUNE extrapolation is performed since MUAP areas should tend to sum more linearly than the MUAP peak amplitudes. In addition, their system provided computer processing and enhanced displays to aid the operator in analyzing the results. Increasingly large responses, evoked by graded stimulation were stored as templates in computer memory. They were then able to derive the waveforms of individual MUAPs by subtracting each template from the next largest. Ballantyne and Hansen went on to use this methodology to study a large number of neuromuscular disorders.

Milner-Brown and Brown (1976) proposed a method for taking alternation into account based on the theoretical firing probabilities of the MUs and exhaustive stimulation to yield as many combinations of MUs as possible. While effective for studying the alternation phenomenon, such methods are impractical in a clinical setting due to the large number of responses required.

Jasechko (1987) took the computer processing proposed by Ballantyne and Hansen a step further by allowing the computer to finely control the stimulator and make the decisions in classifying the evoked responses. Responses were compared by

calculating both the absolute area between response curves and by calculating the Euclidean distance between the vectors of time samples of the responses. Compared to the manual technique, the finer control of the stimulus amplitude, combined with the improved resolution in response classification, considerably reduced the chances of missing CR increments. In an attempt to more accurately calculate MUNE, the individual MUAPs were extracted by successive subtraction of the ranked CR increments, their individual features calculated, averaged, and then divided into the MEP feature. This method assumes a continuous linear summation of MUAP features, as opposed to the piecewise linear model assumed by the original McComas technique.

Cavasin (1989) improved on the Jashechko system by developing a more efficient stimulation control algorithm and implementing a response classification technique based on power spectral features calculated using fast Fourier analysis. By discarding time domain and phase information, these classification features help eliminate problems associated with latency shifting, which will be discussed further in Chapter 5. His MUNE technique, which uses both peak to peak amplitude and absolute area, went back to the original McComas approach of assuming a piecewise linear model. A separate algorithm was also developed to detect and reject instances of alternation in an attempt to ensure that each resulting CR increment is due to the contribution of a single MU. Galea et al. (1991) later used this automated incremental system to obtain and report MUNE for over 100 thenar muscles.

2.6 Measurement of the Contractile Properties of Motor Units

The above studies have shown that M-waves resulting from graded stimuli have unique shapes and are contaminated by very little noise, allowing reliable separation of CR increments into a family of putative MUAPs. The electrical properties of these MUAPs may then be studied and MUNE can be calculated. No attempt, however, was made in the above studies to assess the contractile properties of the associated MUs.

To make the neurophysiological examination of the muscle more complete, it is necessary that EMG investigations be complemented by measurement of the contractile properties of single MUs and of the entire muscle. As noted by McComas (1995), such contractile information should make it possible to determine whether the balance of fast-twitch and slow-twitch motor units has been disturbed, to what extent collateral reinnervation has taken place, and whether the subject is making full use of the contractile muscle mass available.

Data from muscles of different species and within species that differ in function and fiber type composition show a broad range of force capacity, contractile speed, and fatigability (Rafuse et al., 1997). However, due to the challenges associated with measuring in-vivo contractile properties of single human motor units, relatively little corresponding data are available for man. Historically, methods for studying human motor unit contractile properties including spike-triggered averaging, intramuscular stimulation of fine nerve terminals, or percutaneous nerve stimulation (Milner-Brown et al., 1973; Sica and McComas, 1971; Stein et al., 1972; Taylor and Stephens, 1976) usually only allowed a limited number of MU twitch parameters to be measured.

Stein and Yang (1990), using traditional spike-triggered averaging and intramuscular microstimulation coupled with a one-dimensional strain gauge force recording system were able to obtain four independent MUNE's for each site along the median nerve based on the force and EMG recordings from individual thenar MUs. Good agreement was found between the force and EMG methods and with MUNE's calculated using the McComas technique, which was applied at the same stimulation sites but without corresponding force measurements. Force signals were ensemble averaged to improve signal to noise ratios.

Westling et al. (1990) and Thomas et al. (1990; 1991), using intraneural microstimulation as a means of exciting single thenar motor axons within the human median nerve, found a wide range of contractile characteristics in these motor units. A two-axis isometric strain gauge system was employed for force recording. Rigid restraint of the hand and upper limb was required, since respiration, blood pressure pulses and extraneous movement of the subject introduced baseline fluctuations that distorted the strain gauge force measurements. These fluctuations were minimized by synchronizing stimuli to the subject's pulse pressure cycle and resetting the force baseline electronically just before stimulus onset. Single MU force signals could subsequently be recorded without signal averaging.

Around the same time, Eleveld (1992) demonstrated the efficacy of the non-invasive combination of surface stimulation and accelerometry to measure the one-dimensional acceleration response of the first dorsal interosseus (FDI) muscle. Eleveld noted that the acceleration response of a freely moving limb is non-isometric and

therefore cannot be directly compared to an isometric force response such as that obtained from a strain gauge. However, acceleration is proportional to force production, allowing comparison based on correlation of each with standard electrical properties or the distributions of related contractile properties over similar MU samples. Further, due to the inherent AC signal nature of the accelerometer baseline, noise due to respiration of the subject was found to be negligible. As well, blood pressure pulses had little effect since no tissue is compressed between bone and the transducer. As a result, no additional pulse detection or timing circuitry was necessary to obtain reliable results. MUNE's were obtained based on the clustering of acceleration response features into bands representing the incremental activation of single MUs.

Using a methodology and force collection system similar to that of Westling et al., Doherty and Brown (1997) were able to show that the contractile characteristics of single thenar motor units collected using surface stimulation were very similar to those in the earlier intraneural studies by Thomas et al. (1990; 1991) and Westling et al. (1990). Force signals were necessarily ensemble averaged to improve the signal to noise ratio of the resulting twitch responses. An examination of the effects of aging on the electrical and contractile properties these MUs suggested that the human thenar MU pool undergoes significant age-related decrease in MU number, increase in MU size and slowing of contractile speed. Using the same technique, Chan et al. (1998) demonstrated that surface stimulation carries the added advantages of being both noninvasive and lending itself, in some instances, to repeatedly finding the same motor axons at certain

of motor units (typically only 1-3 MUs per subject) is necessarily very time-consuming and fatiguing to the subject. For this reason, such approaches may not be practical in a clinical setting. Furthermore, the intraneural techniques of Westling et al. (1990) are invasive and do not lend themselves to longitudinal study of MUs, while the non-invasive technique of Doherty and Brown (1997) is admittedly biased towards recruiting low stimulus threshold MUs.

2.7 Conclusion

Clearly, a solution is needed which allows the electrical and contractile characteristics of more than several MUs to be obtained in an efficient, non-invasive, single recording session. As noted by McComas (1995), the system should harness the ever increasing power of EMG computers, and use the opportunity to shorten the testing time, to carry out more than one type of mathematical analysis on the same data, and to repeat the test rapidly with some change in the stimulus parameters.

Such a system is presented in the following chapter, which complements the McComas technique and its subsequent improvements with acceleration measurement.

sites along the course of the median nerve, thus allowing longitudinal tracking of their contractile and electrical properties.

Many of the above techniques employ strain gauges. These strain gauges are bonded to metal bars and measure the deflection of the bar due to force produced by the thenar MU. As noted by Eleveld (1992), great sensitivity with adequate signal to noise ratios can be achieved through amplification of strain gauge signals. However, stability of the force measurement is difficult to achieve. Since a baseline passive tension must be applied to the thumb, respiration and blood pressure pulses of the subject can easily corrupt the isometric force recordings of thenar muscles (Westling et al., 1990). This is especially important for small twitches, which may become completely lost in noise due to subject movement or normal tremor. As a result, Stein and Yang (1990) and Doherty and Brown (1997) found it necessary to ensemble average force signals to improve signal to noise ratios. The required synchronization of stimulus to blood pressure pulses significantly complicates stimulus control, necessitating the incorporation of an additionally complicating sensor and timing circuitry to the recording system. Small shifts in subject position will affect the passive tension on the strain gauge, which may cause amplifier saturation if the gain is high. Careful and rigid restraint of the hand and upper limb are therefore required.

The techniques of Westling et al. (1990) and Doherty and Brown (1997) depend on the selection and stimulation of single motor axons in the median nerve that demonstrate activation thresholds significantly separate from those of other axons. To search for and obtain the electrical and contractile properties of even a small population

CHAPTER 3 MEASUREMENT AND ANALYSIS SYSTEM

3.1 Introduction

The system developed for this thesis is capable of measuring and analyzing multiple channels of EMG and acceleration signals simultaneously. Since the thenar MUs produce acceleration of the thumb in both the abduction and flexion planes, a two-axes acceleration measurement system was implemented as in Figure 3.1. This arrangement allows calculation of the direction and magnitude of the resultant acceleration produced by each response. While the system is capable of recording more than one channel of EMG (up to 16 EMG and acceleration channels in total), in the system tests only one channel of thenar EMG was used. The main hardware components of this system are electrodes, accelerometers, amplifiers, a stimulator, and a personal computer equipped with Labview, Matlab and a National Instruments data acquisition board with A/D and D/A capabilities. An overview of the hardware is shown in Figure 3.2. A data acquisition, display and analysis software system was developed based on Labview and Matlab and is discussed in Section 3.2.

3.1.1 Subject Setup

The subjects were comfortably seated and the outstretched hand and arm was held

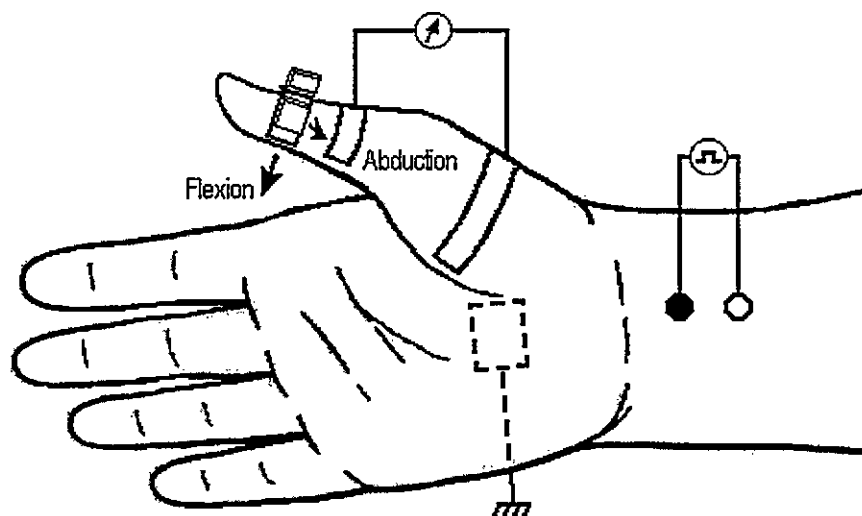
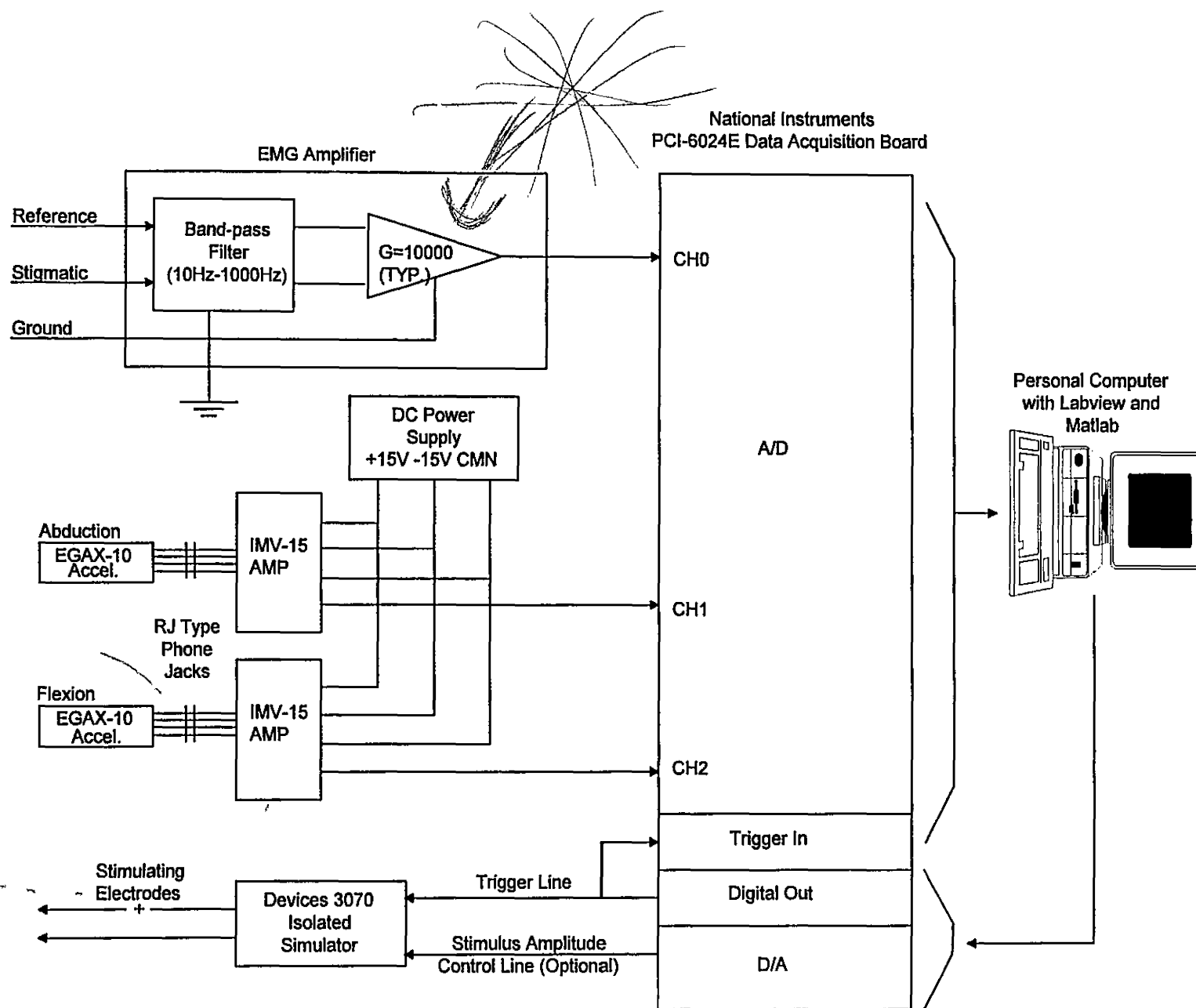


Figure 3.1. Experimental Instrumentation

in the most comfortable, semi-supine position and supported on foam pads to minimize extraneous movement. The padding and non-rigid support of the hand and forearm provided some mechanical decoupling from noise sources such as floor vibration and lab equipment fans. No additional measures were taken to immobilize the hand or forearm, since it was felt that such measures would only make the procedure more uncomfortable and detract from the subject's ability to relax. The importance of subject comfort must be stressed, since it was found through experimentation that successful recording of the minute accelerations being studied depends vitally on the subject remaining relaxed, minimizing movement for up to twenty minutes at a time.

Figure 3.2. Hardware Overview



3.1.2 Electrodes

The EMG recording electrodes were made from disposable, self-adhesive ECG electrodes (Sentry Medical Products, Irvine, CA). The stigmatic electrode was made by cutting the 27 mm by 22 mm electrode longitudinally and mounting the two halves end to end over the thenar eminence to cross the first metacarpal bone perpendicularly at the junction of its proximal and middle thirds as shown in Figure 3.1. The reference and ground electrodes were two halves of an ECG electrode attached over the proximal phalanx of the thumb and the dorsum of the hand respectively. The reference electrode connection was made using fine, braided wire and a lightweight alligator clip, allowing maximum flexibility and minimizing the addition of mass to the thumb.

3.1.3 Accelerometers

The accelerometer chosen for use in this study was the Entran EGAX-10 (Entran Devices, Fairfield, NJ). The unique combination of characteristics of this unit made it well suited to the purposes of this study. The EGAX-10 has a full-scale range of ± 10 g ($1 \text{ g} = 9.8 \text{ m/s}^2$) and built-in overrange protection to ± 10000 g. Experimentation has shown that this range is adequate for thenar studies, since a typical MEP produces a peak-to-peak acceleration signal of approximately 1g. While the extremely high overrange protection of this unit makes it approximately 20% more expensive than comparable units without overrange protection, it is a rugged and reliable miniature accelerometer. Accelerometers with lower overrange protection are easily destroyed by normal handling

such as dropping them on a lab bench or even clipping the leads (Eleveld, 1992). The accelerometers purchased for this study remained reliable and intact throughout the study.

The sensitivity of the device is approximately 8 mV/g with a 15 V excitation. Experimentation has shown that this sensitivity is adequate to measure even the smallest twitches of the thumb, and any higher sensitivity would serve only to amplify background noise. The required 15 V excitation was provided from an accompanying IMV-15 amplifier, which is described later in this section. IMP.

The miniature accelerometer (4 mm X 4 mm X 7 mm) has a mass of 0.5 grams without leads. The small mass of the device allowed for maximum sensitivity while measuring acceleration of the thumb, since little was added to its inertia. More mass added to the thumb would have decreased the acceleration per unit of force produced by the thenar muscle, thus decreasing the sensitivity of measurement. IMP

The frequency response of the EGAX-10 is from DC to 1 kHz (3dB down). Experimentation has shown that there is little information in the acceleration signal produced by the human muscle above 100 Hz (Eleveld, 1992), and therefore the bandwidth of this accelerometer was deemed to be more than adequate. ~~IMP~~

Since accelerations produced by thenar MUs vary widely with respect to their primary vector (Thomas et al., 1990), a two-axes, right-angled acceleration measurement system was employed to allow the magnitude and direction of the acceleration response to be calculated from the abduction and flexion components. Two EGAX-10 accelerometers were glued to a right-angled piece of aluminum, which was then attached over the phalangeal joint to measure acceleration in the abduction and flexion planes as



shown in Figure 3.1. The phalangeal joint was chosen as the mounting position since it provided the best signal to noise ratio during experimentation. Double-sided adhesive strips, designed for attaching electrodes to the skin, were used to mount the assembly in place. The ultra-fine braided leads from the accelerometers were arranged in such a way to provide minimal impedance to the free movement of the thumb.

3.1.4 EMG Amplifier

EMG signals were amplified and band-pass filtered using an A-M Systems 1700 differential EMG amplifier with high-pass and low-pass settings at 10 Hz and 1 kHz respectively. The gain was typically set at 10,000 for collections. For MEP collections the gain was reduced by a factor of 10.

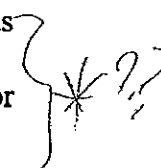
3.1.5 Acceleration Amplifiers

The acceleration signals were amplified using two Entran IMV-15 amplifiers, which had a pass-band of DC to 40 kHz (3dB down). This bandwidth was larger than that of the accelerometer and was therefore more than adequate. The gain of the amplifier was set at 100. The two IMV-15 amplifiers were powered by a single Anatek 2520 DC power supply as shown in Figure 3.2. The IMV-15 amplifiers were designed to pass the necessary 15V excitation voltage to the EGAX-10 accelerometers as well. To provide quick and reliable connections between each accelerometer and its amplifier, each accelerometer-amplifier pair was fitted with male and female RJ type phone jacks,



respectively. Shielding was provided on all wiring for the amplifiers and accelerometers, except for the first 30 centimeters of fine, braided wire leading from each accelerometer.

3.1.6 Stimulator

A Devices 3070 constant voltage isolated stimulator was used for the system. The stimulator was triggered by a pulse on one of the digital output lines from the data acquisition board. The width of the stimulating pulse was set to 50 μ s to minimize the stimulus artifact and subject discomfort. The pulses were applied via 6 mm diameter stainless steel electrodes, mounted 1.8 cm apart on a plastic bar, which was strapped over the median nerve proximal to the wrist. The exact placement of these electrodes was arrived at by searching for the placement that gave the lowest stimulus threshold for thenar motor units with no indication of lumbrical or forearm muscle co-stimulation. 

It was originally intended that the stimulus level would be computer controlled, except for an initial manual search for the MEP and the sub-threshold stimulation levels. In this way, the operator would be removed from the system after finding the MEP and sub-threshold responses. To accomplish this, the Devices 3070 stimulator would be modified as described by Jasechko (1987), and Eleveld (1992), so that it could be computer controlled through the D/A of the data acquisition board, as in Figure 3.2. While the system is capable of controlling this modified stimulator, experimentation showed that for the purposes of this study, manual control of the stimulus level provided a more efficient means of collecting the required responses. The operator was capable of efficiently determining which levels of stimulation needed to be explored in order that no

composite responses were missed and a sufficient number of clean acceleration responses were gathered at each level. If automation of this process were desired, the stimulator would be replaced by the modified version as described by Jasechko and Eleveld.

3.1.7 Data Acquisition Board

All signals were sampled at 4000 Hz and collected by a National Instruments PCI-6024E data acquisition board. The board was plugged into a PCI slot of the personal computer. Using direct memory addressing, the board can guarantee 200 kS/s, which accommodates the demands of our three-channel, 4 kHz system configuration easily. The board can accommodate up to 16 single ended or 8 differential channels of A/D, up to 8 digital I/O lines and two TTL compatible trigger lines. The EMG signal was collected on Channel 0 of the A/D, the abduction acceleration signal was collected on Channel 1, and the flexion acceleration signal was collected on Channel 2, as shown in Figure 3.2. All A/D channels were configured for -5 to 5 volt operation, with a unitary gain. D/A Channel 0 was used to set the stimulus amplitude, Counter 0 was used to trigger the stimulator from Labview, while PFIO/Trig line 0 was used to synchronize the data collection to the stimulation event. The 12-bit analog to digital converter of this board provided an overall system resolution of 0.244 μV for EMG signals and 3.0 mg ($1 \text{ mg} = .0098 \text{ m/s}^2$) for acceleration signals, assuming gains of 10,000 and 100 respectively.

Detailed information about the capabilities and specifications of the PCI-6024E board can be found in the National Instruments PCI-6024E User Manual. (National Instruments Inc., 1998)

3.1.8 Personal Computer

The system was implemented on a 166 MHz Pentium PC with 64 MB of RAM and a 4GB hard drive running Windows 95. This machine proved to be adequate for running the system with extensive online processing taking place, as described in the software section to follow. The Labview 5.1 Full Development System was installed with the accompanying Ni-DAQ drivers for the PCI-6024E data acquisition board. Also, Matlab 5.2 was installed, along with its wavelet toolbox, so that online decompositions could be performed from Labview using simple Matlab scripts.

3.2 Software

The software portion of this system was programmed using the Labview 5.1 Full Development System. Labview was chosen for this project since it provided a state-of-the-art graphically oriented programming language which could expose the full functionality of the data acquisition board, while providing a comprehensive library of pre-programmed functions called VIs (Visual Interfaces). These functions included I/O, signal processing, statistics, mathematics, string handling, file manipulation and graphing functions. The package facilitated the rapid development of a highly powerful and flexible data acquisition and analysis application. The graphical user interface (GUI), during a typical recording session, is shown in Figure 3.3.

The software is based on the McComas incremental counting technique, which was first automated by Jasechko (1987) and later modified by Cavasin (1989). Many of

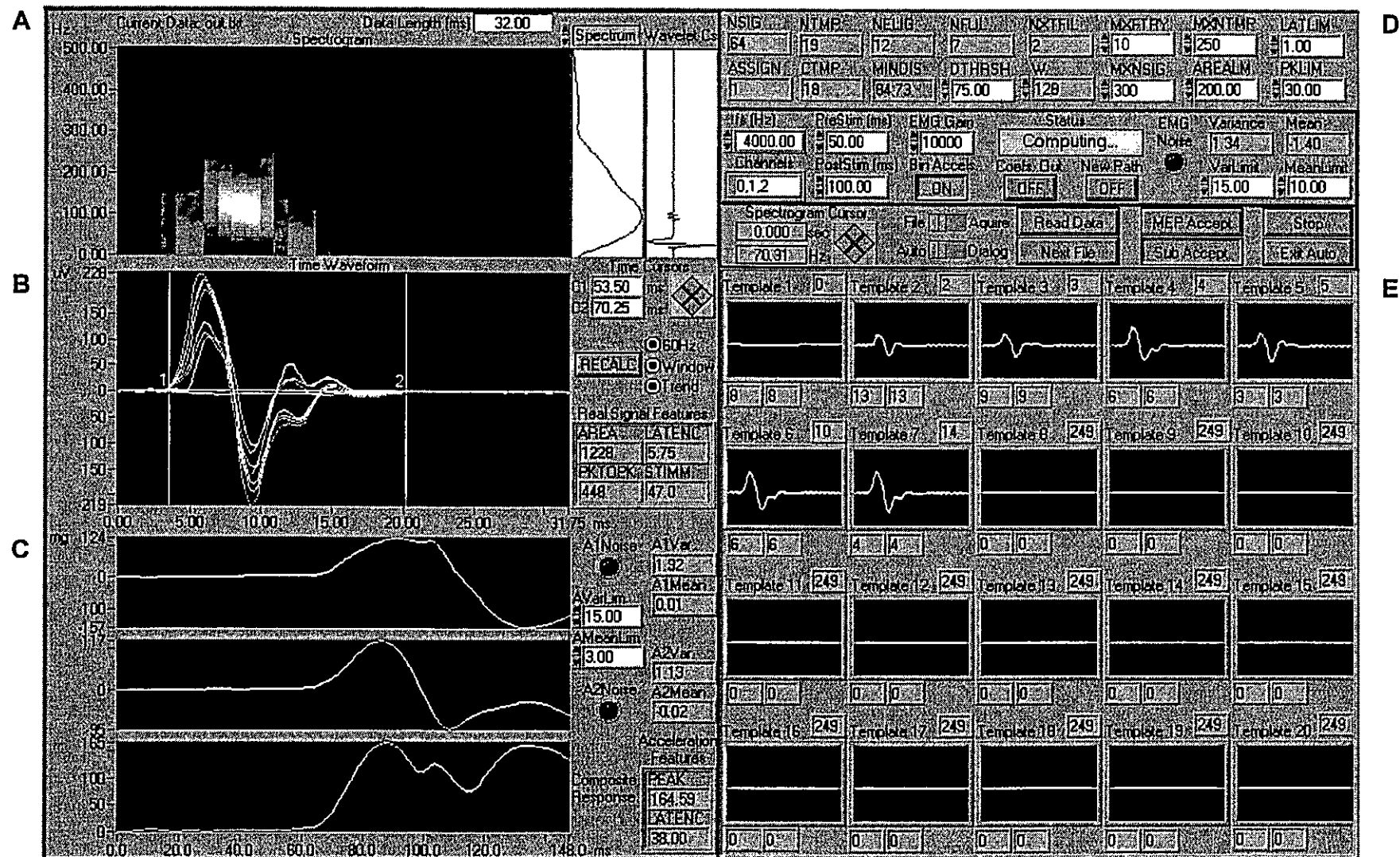


Figure 3.3. Graphical User Interface. *A*: Signal decomposition coefficients. *B*: EMG waveform (CR) and signal processing. *C*: acceleration responses (abduction, flexion and summated). *D*: system parameters and controls. *E*: M-wave templates and acceleration response counts.

the algorithms described in this section have been retained or modified from these systems. The software flowchart is shown in Figure 3.4, and the response classification flowchart, which is called at various points of the software flowchart, is shown in Figure 3.5.

3.2.1 System Parameters and Initialization

Almost every parameter used in the system is software selectable and in most cases can be changed on-line through the graphical interface, even in the middle of a recording session. Parameter values that work well for the average thenar are empirically determined and saved as defaults. When the program is subsequently run, these defaults are automatically loaded and all variables are initialized accordingly. With appropriate adjustments to the parameters and utilization of additional recording channels, this system can easily be adapted to study muscle groups other than the human thenar.

3.2.2 Acquire

A sub-VI named Acquire was written to handle the I/O tasks of stimulus level setting, stimulus triggering and data collection. The built-in functionality of Labview allows these tasks to be carried out in a flexible and reliable manner. Two segments of EMG and acceleration data are collected by the Acquire sub-VI, as shown in Figure 3.6. The first segment is collected immediately before the application of the stimulus and the second immediately following it. The first segment is used to determine pre-stimulus

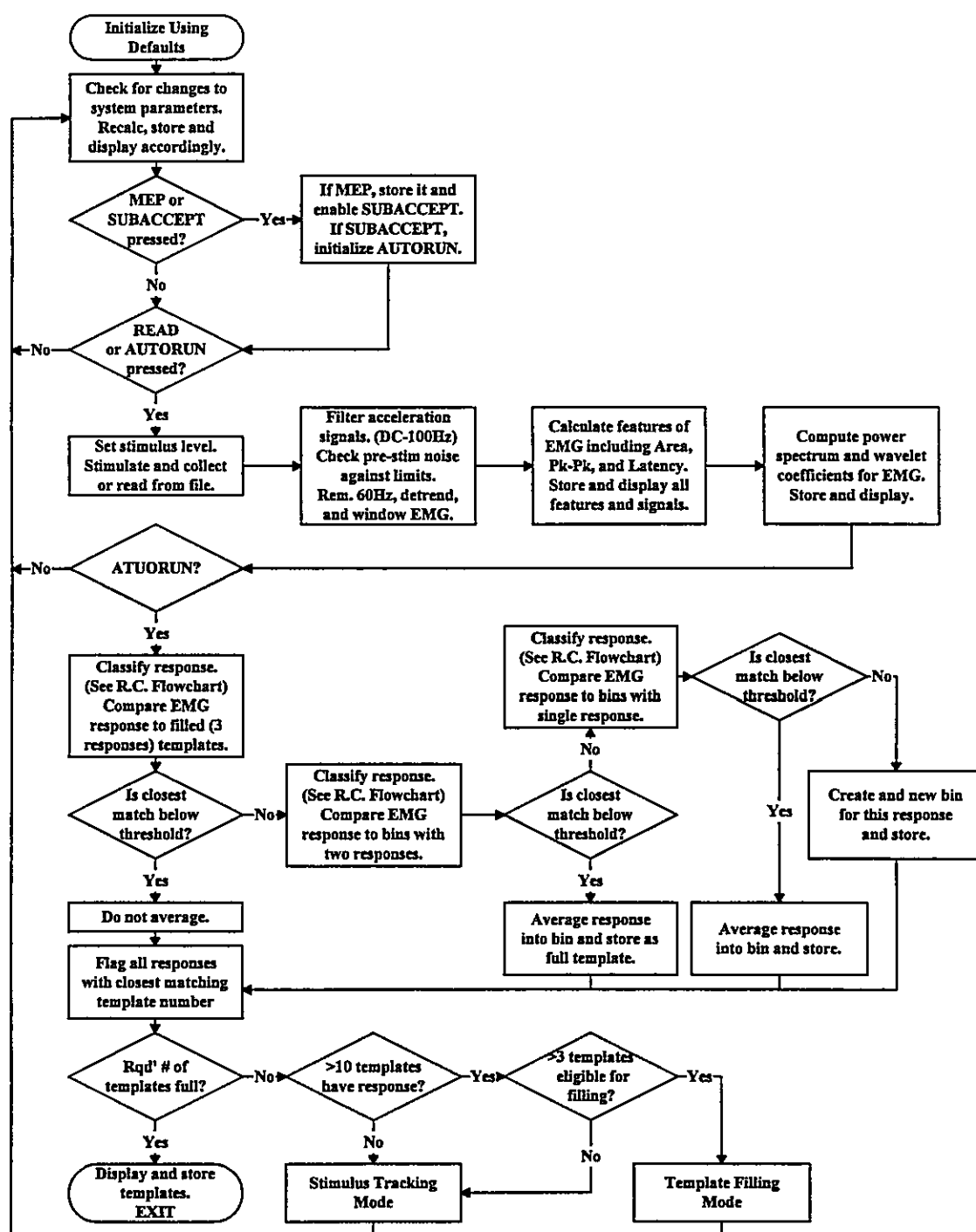


Figure 3.4. Software Flowchart

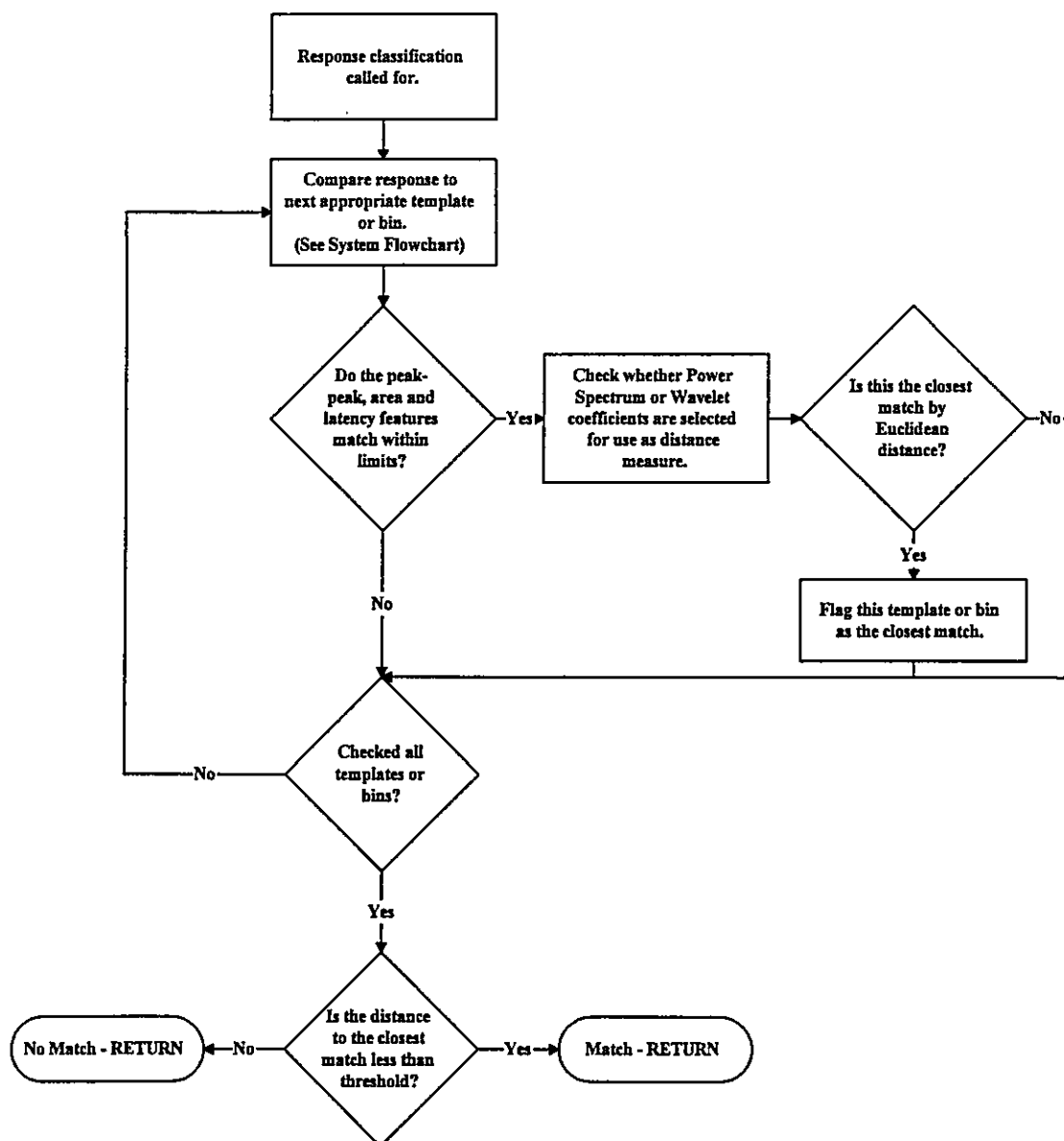


Figure 3.5. Response Classification Flowchart

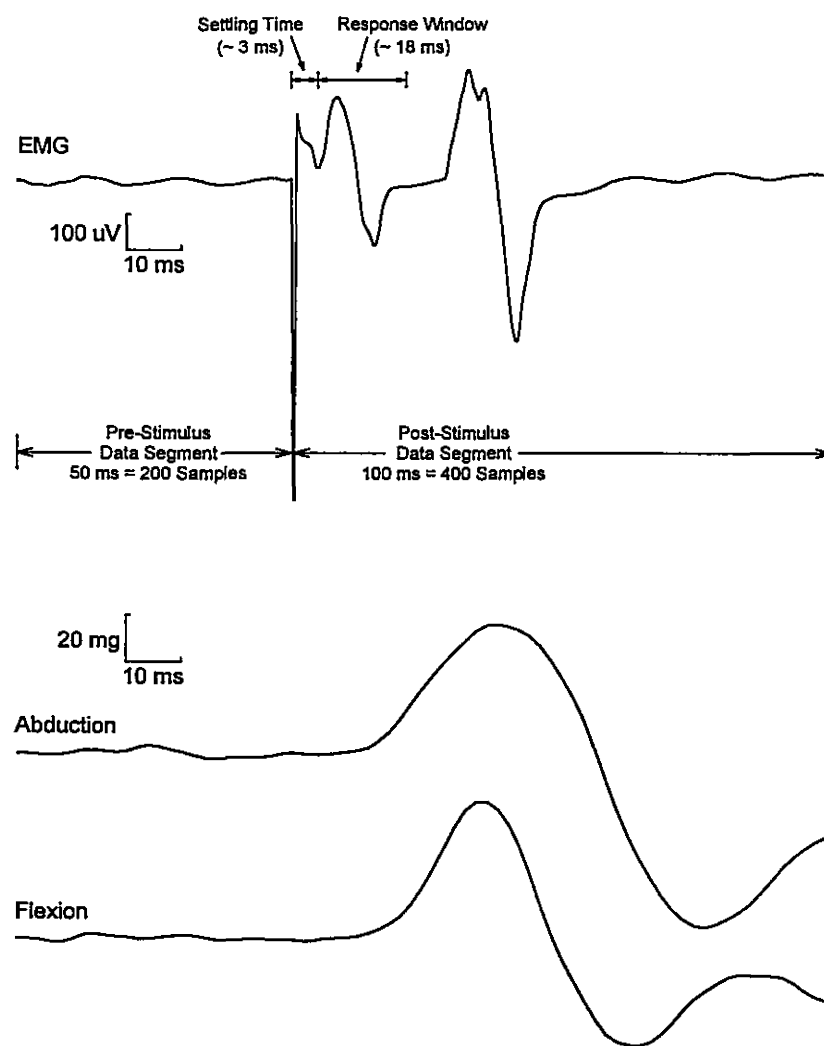


Figure 3.6. Signal Epochs

noise and baseline levels for the EMG and acceleration responses. The second segment contains the stimulus artifact and evoked responses.

Parameters from the main VI are passed to Acquire as it is called. Key parameters (and settings) include stimulus level, data acquisition channel numbers (0,1,2), sampling frequency (4000 Hz), pre-stimulus scan duration (50 ms) and post-stimulus scan duration (typically 100 ms). Upon calling Acquire, the stimulus level is set by placing the appropriate voltage on D/A Channel 0. The acquisition routine is then initialized and begins buffering scans of the input channels. A delayed pulse is then sent to trigger the stimulator and acquisition routine simultaneously. This trigger pulse is detected by the acquisition routine on the PFI0/Trig line. The delay in the trigger pulse is necessary to allow the acquisition routine to initialize and buffer enough scans of pre-stimulus data before the stimulus occurs. Due to the fact that Windows is not a real time operating system, the initialization time varies for the acquisition routine, and it was found through experimentation that the trigger pulse needed to be delayed more than 100 ms to ensure desired operation.

When the data acquisition is complete, the resulting 1000-sample by 3-channel data array is stored in memory for use in the main program.

3.2.3 Read From File

To facilitate post-processing and reenactment of entire recording sessions, the operator has the option to read responses from files stored on the computer from previous recording sessions. If this option is selected, the Acquire algorithm is replaced with a

text file reading function that returns response data in exactly the same format as Acquire, to the same arrays. The only difference is the source of the data.

This option is crucial for development and research, as it allows the operator to try an unlimited number of parameter and system configurations with the same data set. The live subject is needed only once, for the original recording sequence, and post-processing can be done at a much higher or lower speed, depending on the computational demands of the study.

1

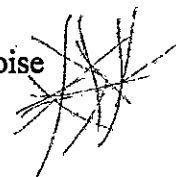
3.2.4 Signal Processing

The processing described in this section is optionally applied to every signal sampled by the system, whether read from a data file, recorded alone or as part of an automated template recognition sequence. All techniques are optional and associated parameters are software selectable to allow for online experimentation.

3.2.4.1 EMG 60-Hz Noise

Ever present in EMG studies such as this one is the problem of dealing with differential 60-Hz noise picked up by the recording electrodes due to capacitive coupling of power lines and equipment power sources to the subject's skin and transducer leads. A typical pre-processing EMG signal is shown in Figure 3.7 (A). The original signal contains significant levels of 60-Hz noise.

Since M-wave responses contain a significant amount of information in the 60-Hz frequency range, most filtering techniques aimed at removing only the 60-Hz noise



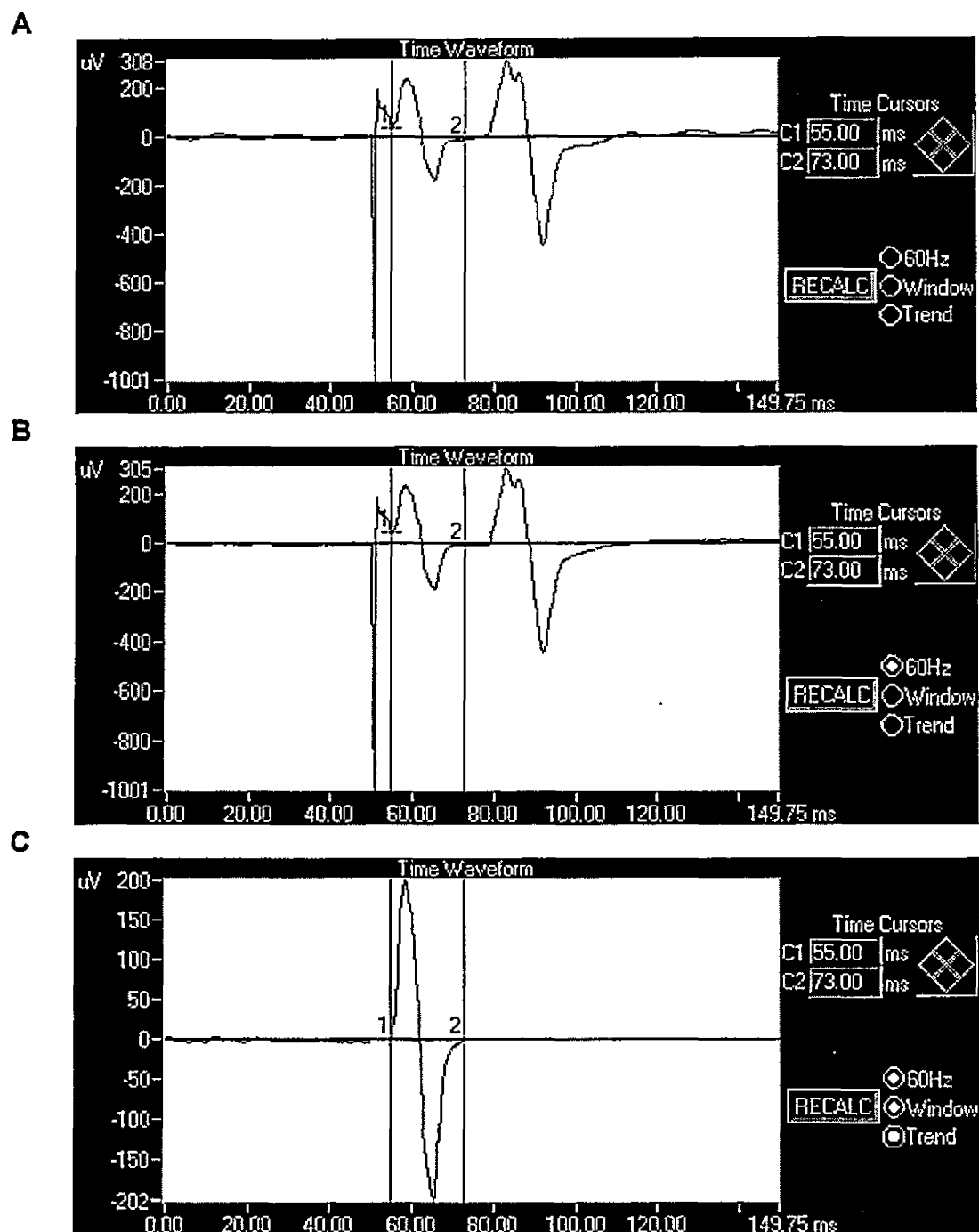


Figure 3.7. EMG Signal Processing. *A*: Original signal. *B*: after 60-Hz reduction. *C*: after windowing and de-trending.

produce unsatisfactory results. Digital notch filtering, a method chosen by some to reduce 60-Hz to appropriate levels, was ruled out for this study due to the "ringing" phenomenon associated with it (Slawnych et al, 1996). Instead, a template of the 60-Hz noise is constructed using the pre-stimulus segment of EMG data, and this template is then subtracted from both the pre- and post-stimulus segments to remove the noise.

To construct a 60-Hz template with the correct phase and amplitude, an iterative-difference approach is used to match the phase and then the amplitude of the template to the 60-Hz contained in the recorded pre-stimulus segment. The difference between the pre-stimulus segment and an identical length 60-Hz sine wave template, shifted in 1-degree increments from 0 to 359 degrees, is found at each iteration. The phase at which this difference is a minimum is used as the phase of the 60-Hz template. Holding the phase constant at this level, the appropriate peak amplitude of the 60-Hz template is determined in the same manner. Beginning with a peak amplitude of 1.44 times the variance of the pre-stimulus data segment, the difference between the pre-stimulus segment and the identical length 60-Hz template is determined at each iteration, while reducing the peak amplitude of the template to zero in 1-percent increments. The amplitude at which this difference is a minimum is used as the amplitude of the 60-Hz template.

Since it is reasonable to assume that this 60-Hz template is representative of 60-Hz noise contained in the post-stimulation data segment as well, the template is subtracted from both the pre- and post-stimulation segments, reducing 60-Hz noise in the

entire EMG signal. This method was found to be extremely satisfactory as seen in the before (A) and after (B) example of 60-Hz template subtraction shown in Figure 3.7.

3.2.4.2 EMG Stimulus Artifact and Baseline Detrending



The post-stimulus data segment, which contains the stimulus artifact and M-wave response, is windowed to a user selectable length of approximately 18 ms following a user selectable settling time of approximately 3 ms as shown in Figure 3.6. The window is user defined with cursors while examining the MEP signal. It was found that using the MEP to define the response window allowed for variable response latency while removing most of the stimulus artifact. By setting the response window to approximately 18 ms, the inclusion of an F-wave or H-wave in the response is avoided, as shown in Figure 3.6.

Even after windowing out the majority of stimulus artifact, the M-wave responses are typically superimposed on a remaining slowly decaying baseline artifact. Since the system relies on the application of Fourier and wavelet transforms, this baseline must be removed to prevent leakage due to the endpoints of the signal not being equal to zero. This preconditioning is accomplished by subtracting a line interpolated from the first point to the last point of the response window. This method was found to introduce little signal distortion when used with an appropriate user-selected window. Figure 3.7 shows the signal before (B) and after (C) windowing and de-trending.

3.2.4.3 Acceleration Noise Sources

Acceleration signal baseline fluctuations due to extraneous subject movement, respiration and blood pressure pulses are minimized due to the self-leveling nature of the accelerometers. If the limb changes position slightly, the accelerometers indicate this shift, but return to their original baselines when the subject stops moving.

However, due to small DC offsets built into the accelerometers, the baselines are not exactly zero. Although the accelerometers are temperature compensated for accurate measurement over a wide range of temperatures, the baseline moves significantly with change in temperature. For these reasons, the baseline of each recorded acceleration signal is zeroed in software by calculating and subtracting the average offset during the pre-stimulus window. This zeroing removes built-in electronic and temperature offsets, as well as any other slowly changing baseline effects.

Baseline fluctuations due to respiration were further minimized by asking the subject to keep their breathing as calm and smooth as possible. No attempt was made to avoid pulse pressure waves, since their effects on acceleration responses were found to be negligible by Eleveld (1992). While pulse pressure waves are a significant source of noise for force studies using strain gauges (Westling et al., 1990), the accelerometers place no abnormal resting pressure on blood vessels of the thumb, thus avoiding the problem of movement caused by blood pressure pulses in compressed tissue.

The most significant acceleration noise sources are those transmitted mechanically from the environment and apparatus to the subject, and the movement of the subject caused by involuntary nervous action of the upper body, arm and hand

muscles. Foam pads were used to decouple mechanical noise sources transmitted through the table that the subject's arm rested on. Subject concentration and relaxation were the only methods used to lower the contribution of involuntary muscle activity noise. Since it is impossible for every recorded acceleration response to be noise-free, a screening criterion was established. Excessively noisy signals were discarded using the rejection criteria outlined below.

3.2.4.4 Acceleration Filtering and Composite Response

As shown by Eleveld (1992), there is little significant information in the acceleration signals produced by human hand muscles above 100 Hz. To remove the high frequency noise above this level, the acceleration signals are low-pass filtered in software using a digital fifth-order butterworth filter with a cutoff frequency of 100 Hz. In addition, the signals are decimated by a factor of 8 to reduce memory and disk storage requirements without loss of signal information.

The perpendicular abduction and flexion components of acceleration are summated using the Pythagorean theorem to determine the prime vector of acceleration at each time step. The amplitude of the resultant acceleration vector is calculated by taking the square root of the sum of squares of the abduction and flexion amplitudes. The resultant composite response is displayed on the graphical user interface below the abduction and flexion signals, as shown in Figure 3.3 (C).

3.2.4.5 Unacceptable Responses and Averaging

The pre-stimulus EMG and acceleration response segments are used to assess the level of background noise due to muscle activity and extraneous movement. If the variance of the pre-stimulus samples of any M-wave or AR exceeds empirically determined limits, the noise is deemed to be excessive and the signal is discarded.

The M-waves resulting from graded stimuli have unique shapes and are contaminated by very little noise, allowing reliable separation into a family of templates using the methods described later in this chapter. Very few M-waves need to be discarded due to noise. However, their associated acceleration responses have very similar shapes and individually, exhibit relatively poor signal to noise ratios due to extraneous movement such as normal tremor.

With the subject relaxed, the overall noise in the recording system is 5 μ V peak-to-peak for EMG and 5 mg peak-to-peak for acceleration signals. The average peak-to-peak MUAP recorded for this thesis was 70 μ V, while the average MU acceleration response had a peak of 13 mg. This means that the average signal to noise ratio of the recorded MUAPs was approximately 14 (23 db), while the average MU AR had a relatively poor signal to noise ratio of less than 3 (9.5 db).

Assuming that the noise present in each response is uncorrelated from stimulus to stimulus and with twitch response, all acceptable ARs associated with each CR template are ensemble averaged, thus improving the overall signal to noise ratio for MU ARs.

During the recording session, a significant proportion of acceleration signals exceed the empirically determined pre-stimulus noise threshold level and must be

discarded. Noisy responses trigger red indicator lights on the GUI, which are displayed to the subject as feedback to promote relaxation. It was found through experimentation that this feedback system works well to help subjects calm their extraneous movements during recording sessions, thus improving the yield of clean ARs.

3.2.4.6 Signal Feature Extraction

After performing noise reduction, windowing and detrending, a number of parameters of the EMG and acceleration signals are calculated, displayed and stored. EMG signal parameters including area under the curve ($\mu\text{V}\cdot\text{ms}$), peak-to-peak amplitude (μV) and peak latency (ms) are calculated. Acceleration parameters including positive peak amplitude and peak latency are calculated based on the resultant acceleration signal, which is composed of both abduction and flexion components as described above. When automated stimulation is used, the stimulation level used to evoke the response is also stored as part of the signal parameter set. All parameters are displayed on screen and stored for later use in the template recognition algorithm.

3.2.4.7 Fourier and Wavelet Transforms

Fourier and wavelet transforms of the M-wave are calculated and the coefficients are stored for use in signal reconstruction and as response classification features. The first 128 points (32 ms) of the M-wave (after preconditioning) are fed to the Labview Real FFT VI, which uses a standard decimation in time algorithm to produce 128 complex Fourier coefficients. The same 128 points are fed to a Matlab script box, which

causes Matlab to perform a level 3, 'db5' wavelet decomposition of the M-wave (Misiti et al., 1996), returning 152 wavelet coefficients to Labview. These methods of analysis are discussed in Chapter 5.

Due to the bandlimited nature of EMG signals as discussed by Cavasin (1989) and others, only the magnitudes of the 2nd to 21st Fourier coefficients corresponding to frequencies between 15 Hz and 330 Hz are retained as spectral response features for use in the template recognition algorithm. Instead of storing all 128 data points for each CR increment, the 1st through 21st Fourier coefficients are stored for use in reconstruction and combination of templates at a later stage. Similarly, the wavelet decomposition is performed at such a level as to obtain only those coefficients containing significant information. A study of the information contained in the spectrum and wavelet coefficients and their utility in M-wave pattern recognition can be found in Chapter 5.

3.2.5 Recording Session Protocol

The experimental protocol consists of instrumenting the subject, testing the placement of electrodes with the stimulator under manual control, making any necessary instrumentation adjustments, acquiring the MEP and sub-threshold responses, and adjusting the stimulation level for the duration of the automated recording sequence. Informed consent was obtained in all cases prior to examination of subjects.

3.2.5.1 Instrumentation

The subject assumed a comfortable seating position and was instrumented as described earlier in the chapter. The optimum stimulus electrode placement was determined with the stimulator under manual control while observing responses on the GUI, as shown in Figure 3.3 (B). The exact placement of the stimulating bar was arrived at by searching for the placement that gave the lowest stimulus threshold for thenar motor units with no indication of lumbrical or forearm muscle co-stimulation. The stimulating bar was held in place using an adjustable strap. The subject was asked to relax and keep movement to a minimum during the recording session. The subject was also asked to watch the AR noise threshold indicators on the GUI, and use them as feedback to achieve sufficient relaxation.



3.2.5.2 MEP Acquisition

The MEP and corresponding ARs are first collected and stored. The operator manually increases the stimulus amplitude, pressing "READ DATA" at regular intervals to trigger the collection system, until no increase in the size of the response is observed. At this stimulation level the M-wave is deemed to contain the summated response of all the MUs in the muscle, and upon acquiring corresponding ARs below the noise threshold, the "MEP ACCEPT" button, as shown in Figure 3.3 (D), is pressed to store the MEP responses.

As noted by Cavasin (1989), finding the optimum stimulating bar placement and acquiring the MEP manually before automated recording of other CR increments offers several advantages:

- 1) The most uncomfortable part of the recording session is completed first, allowing the subject to relax during the acquisition of the much lower stimulus level M-waves, resulting in fewer signal rejections due to excessive noise.
- 2) The windowing cursors can be manually placed at the clearly defined beginning and end of the MEP response, ensuring that all M-waves fall within the set window.
- 3) A poor recording electrode placement resulting in degraded signals can be quickly recognized and corrected by examining the MEP amplitude and area.
- 4) A poor stimulating electrode placement resulting in excessively high stimulus threshold for the MEP can immediately be discovered and remedied.

3.2.5.3 Sub-Threshold Acquisition

Before initiating automatic collection of CR increments and corresponding ARs, the sub-threshold stimulation level must be found. The operator finds a stimulus level just below the threshold of the first MU by observing the recorded M-wave and ARs while manually triggering the collection system at appropriate stimulation levels. Sub-threshold stimulation evokes no EMG or acceleration responses. Marginally higher stimulus intensities reach threshold, and all-or-nothing EMG and acceleration responses appear simultaneously. When the sub-threshold stimulation level is found, the response

is accepted by pressing the "SUB ACCEPT" button on the GUI. This response is the baseline at which the collection begins.

Pressing the "SUB ACCEPT" button initializes all variables and arrays required for the automatic collection algorithm, storing the sub-threshold response as the first signal of the first template. The corresponding ARs are stored in separate arrays with an indication of which CR increment they belong to for the duration of the session. "AUTORUN", as shown on Figure 3.3 (D), is set to true, and the complete software loop is repeated until:

- 1) "EXIT AUTO" is pressed.
- 2) The desired number of templates is filled.
- 3) The area of the largest template collected exceeds 80% of the MEP area.

3.2.6 Response Collection

After the MEP and sub-threshold responses are confirmed, the software automatically stimulates, collects and classifies responses at a rate of 1 Hz, while the operator manually controls the stimulus amplitude. As discussed previously in this chapter, manual control of the stimulus level proved to be most efficient for collecting sufficient numbers of noise-free responses at all levels.

The operator typically keeps the stimulus at a sub-threshold level until several examples of the baseline response are collected. The stimulus level is then gradually increased and decreased in such a fashion as to collect sufficient numbers of noise-free responses at each CR level, while making sure not to miss any CR increments along the

way. Increasing stimulus intensities result in incremental EMG and acceleration responses, indicating additional motor units are being successively excited. When the stimulus level is decreased, these response phases appear in reverse order.

To assist the operator in collecting sufficient numbers of responses at each increment, the GUI provides extensive feedback during the response collection session. On the 'Time Waveform' graph, the most recently collected M-wave is shown in green, while all previously filled templates are shown in white. By comparing the current response to previously filled templates, the operator can easily determine which CR levels need further exploration, and can verify that no repeatable increments exist between templates.

Current acceleration responses and their pre-stimulus noise statistics are shown, as well as the composite acceleration response. Each individual filled template (with at least three responses) is also shown in the lower-right portion of the GUI (Figure 3.3 (E)), with corresponding clean AR counts for both abduction and flexion signals. These counters help the operator determine which CR levels need to be repeated in order to collect sufficient number of noise-free ARs corresponding to each template.

3.2.7 Response Classification

As each response is collected it is compared with previously collected CR increments in an attempt to classify M-waves produced by identical MUs into templates. Prior to classification, all M-waves undergo the signal processing described previously in this chapter. Response classification is based upon the M-waves as opposed to the ARs,

due to the relatively noise-free and unique characteristics of surface recorded MUAPs. All discussion in this section is therefore concerned with the M-waves and CR increments and it is assumed that the corresponding ARs are indexed and stored appropriately.

M-waves that match no previously collected responses are stored in temporary save bins, while matching responses are averaged into templates, as shown in the software flowchart of Figure 3.4. The response classification protocol is summarized in Figure 3.5. This protocol is called at several points in the software flowchart to compare the present M-wave to previously stored templates and save bins. To reduce unnecessary computation time, the pattern recognition system screens responses by comparing their peak-to-peak amplitudes, areas, and latencies to existing templates and save bins. Matching of a M-wave to a template or save bin is immediately failed if any difference beyond the limits of 30 uV peak to peak, 200 $\mu\text{V} \cdot \text{ms}$ area, or 1 ms latency exists.

The responses are classified using a template comparison of the power spectral or wavelet features of the M-wave response and previously collected templates or save bins based on the Euclidean distance measure:

$$D_s = \sqrt{\frac{\sum_{j=1}^N [C_R(j) - C_T(j)]^2}{N}}$$

where, N = number of features (20 spectral features or 152 wavelet features)

$C_R(j)$ = spectral/wavelet features of the response

$C_T(j)$ = spectral/wavelet features of the template or save bin

The software accommodates the use of either spectral or wavelet features as selected by a switch on the GUI. Spectral features were used for response classification in the six thenar studies presented in this thesis with the discrimination threshold set at 75 for all studies. This value agrees with that used by Cavasin (1989) and was decided upon after completing the study of spectral and wavelet features detailed in Chapter 5.

As outlined in the software flowchart, each response is first compared to existing full templates using the criteria outlined above. A template is deemed to be full when it contains three matching responses. If the distance measure between the current response and the closest matching full template falls below the discrimination threshold, the response is stored as a match of that template. If the response does not match an existing template, it is compared to responses stored in save bins by the same criteria. If the response matches a save bin it is averaged into that bin. A save bin becomes a full template when it contains three members. If there is no match among previously collected templates or save bins the response is assigned to a new save bin.

Full templates are displayed on the bottom right portion of the GUI, as shown in Figure 3.3 (E). Above each individual template graph, the template's position in the template array is shown. The numbers of clean abduction and flexion responses that have been collected for each template are displayed below each template's graph.

3.2.8 Session Termination

The recording session is not terminated before ten templates have been filled and satisfactory numbers of clean ARs have been collected for those templates. Above the

level of ten templates, recording may be continued until excessive alternation obviously presents itself. An example of the first few M-wave templates and associated acceleration responses resulting from a typical recording session is shown in Figure 3.8. Only the smallest 6 of 14 templates are shown for clarity.

3.2.9 Response Storage

Once a recording session is completed, several output files are created in comma-separated-variable (CSV) format, so that the session data may be imported to a spreadsheet for analysis.

The first output file contains all raw data acquired from the three input channels for every stimulus of the recording session. Identifying information is added between signal sets to include signal number, stimulation level, and template classification information. An entire session can be reenacted an unlimited number of times once this raw data is saved to disk, using the 'read from file' capabilities of the software. In this way, multiple parameter sets, classification schemes and signal processing methods can be tested and analyzed using the same data set.

A second CSV file contains the CR templates sorted in order of decreasing peak to peak amplitude. Each 128-point template is tagged with its position in the template array so that it may be cross-referenced to its associated ARs.

The third and fourth CSV files contain abduction and flexion ARs, respectively. Only ARs with pre-stimulus noise levels below the threshold, which are associated with

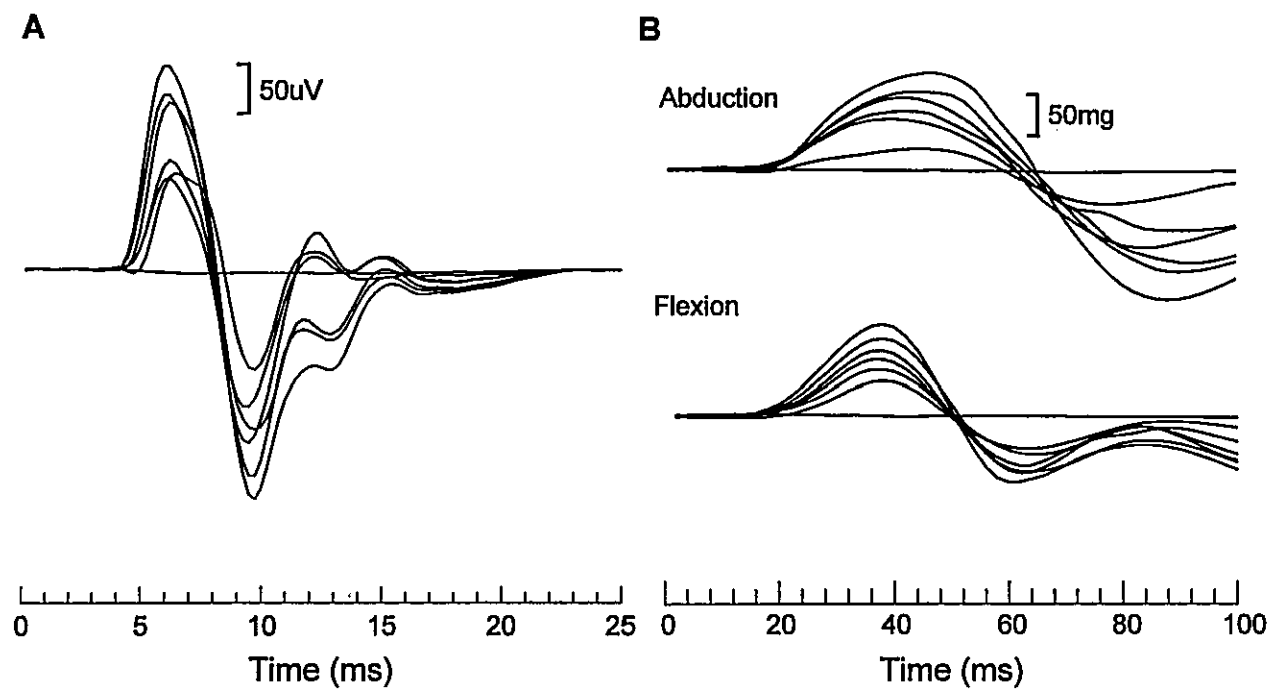


Figure 3.8. Smallest 6 of 14 M-wave templates (A) and associated acceleration responses (B) recorded from a human thenar muscle.

full CR templates are saved to file. The responses are tagged, grouped and sorted in order of increasing position in the corresponding template array.

The fifth CSV output file, which can be used to analyze various template classification techniques, contains the response window of every collected M-wave and their corresponding spectrum and wavelet coefficients calculated during the session. Signal identification and classification information based on current software settings is appended, as well as signal features including peak-to-peak, area and latency. This plethora of information about the individual responses, exported in a one-M-wave-per-spreadsheet-row format, facilitates a detailed study of the recorded M-waves and various classification techniques applied to them.

CHAPTER 4

EMG and Acceleration Signals

4.1 Thenar Studies

A study was conducted using the left and right thenars of three healthy male volunteers, 25, 26 and 55 years of age. The objective of the six thenar studies detailed in this chapter was to demonstrate the utility of the presented system in recording and decomposing M-waves and their associated ARs into putative MUAPs and MU ARs. To test the validity of the resulting putative responses, their electrical and contractile characteristics were analyzed and compared with those found in similar physiological studies.

Mean values and standard deviations are given along with median values to help illustrate skew in distributions. Comparisons between mean values were made with two-tailed *t* tests, and relationships between variables were analyzed with linear regression. Probability values $P < 0.05$ were regarded as statistically significant.

4.2 All-or-Nothing Response of M-Waves

M-waves resulting from graded stimuli have unique shapes and sizes and demonstrate high signal to noise ratios. As noted by Doherty and Brown (1993), the evidence that a single motor axon can be successfully excited independent of any other motor axons with surface, bipolar stimulation may be considered established based on the

fractionation of the single MUAP recorded with either surface or intramuscular electrodes, which would indicate the stimulation of two or more axons. As additional MUs are added to and removed from the response by changes in stimulus level, the 'signature' of the related surface detected potentials are unique in shape and size and can readily be identified using visual or automated pattern recognition. This uniqueness of shape may be expected, given the differences in location, depth, and orientation of the various MU endplate zones within the thenar muscles with respect to the surface recording electrodes. The system described in the present study uses this premise to automatically resolve responses elicited from repeated activation of distinct motor unit sets into templates, while storing all of the associated acceleration responses for further analysis.

4.3 Alternation

While the firing of a MU is an all-or-nothing event, MU thresholds can vary over time. Over a small stimulus voltage range, we must therefore speak of the probability that a MU will fire varying from 0 to 100% (Slawnych et al, 1996). The shape of this probability curve is generally assumed to be 'S' shaped as shown for five hypothetical MUs in Figure 4.1 (A). At stimulation level 'S₁', the probability of MU₁ being activated is 0%, while at stimulation level 'S₂', MU₁ will be excited 100% of the time. In the stimulus range 'P', the probability of activation for MU₁ varies from 0 to 100%.

Alternation, also known as probabilistic activation, refers to a group of MUs firing in diverse combinations to produce more CR increments than there are MUs

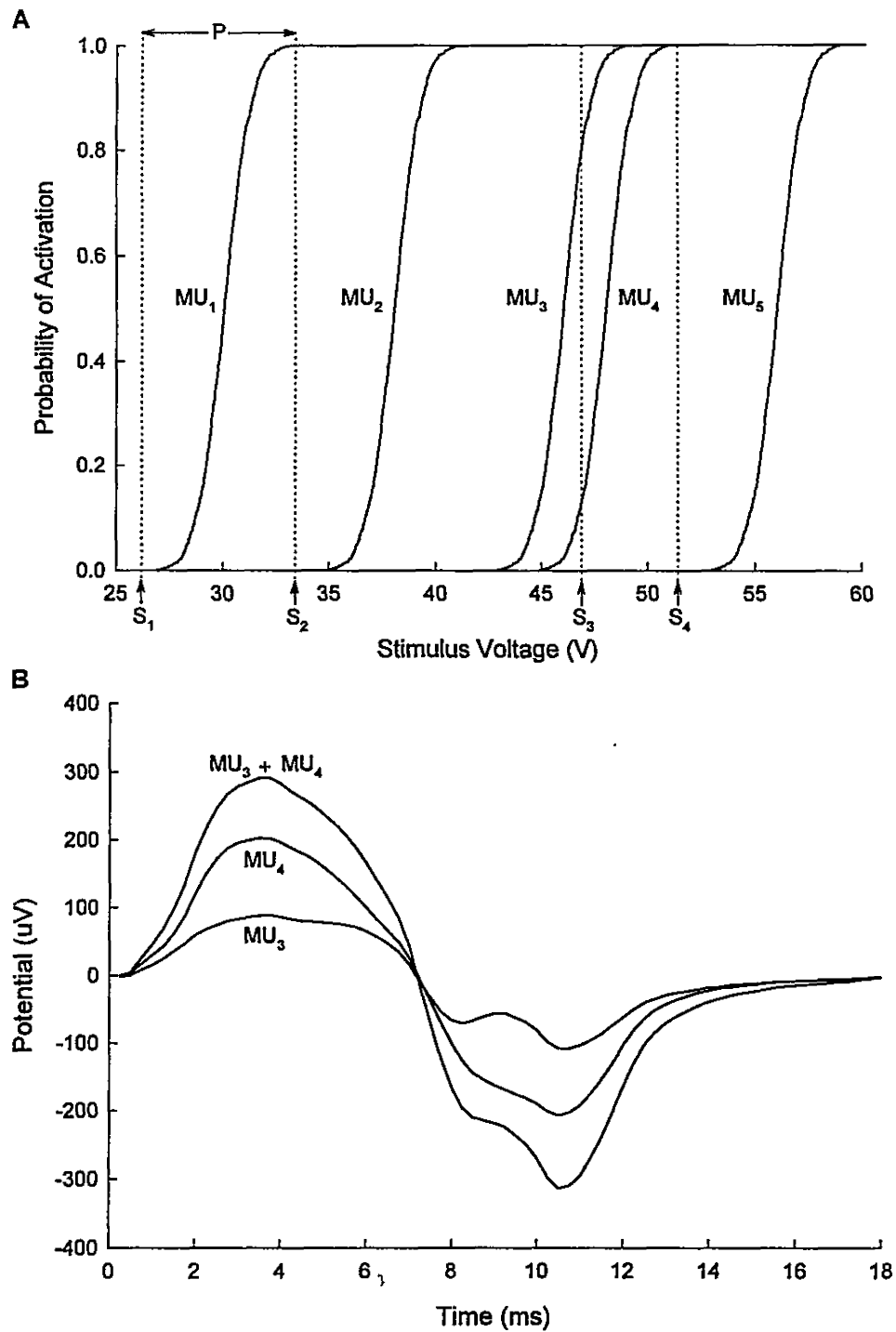


Figure 4.1. Alternation. *A*: Activation probability curves. *B*: alternation example at stimulus level S_3 . The signals already include MU_1 and MU_2 .

(McComas et. al., 1971). This is a result of multiple MUs having overlapping probability of activation curves as illustrated for MU₃ and MU₄, in Figure 4.1 (A). As illustrated in Figure 4.1 (B), these two MUs can produce up to three different responses. When larger numbers of MUs have overlapping activation probability curves, the number of possible M-waves increases. Without some method of detecting these occurrences, each CR increment would be incorrectly attributed to the addition of another MU. Alternation would therefore result in an overestimate of the MUNE and a general skew towards smaller electrical and contractile properties for the average MU in a given sample.

Fortunately, following the probabilistic activation premise, it is highly unlikely that the responses of two MUs firing in unison will be mistaken for a single MUAP upon repeated stimulation with finely graded incremental stimuli. Consequently, it is reasonably certain that the first response increment in the CR above the baseline will represent the response of a single MU. However, while the first few MUs are generally activated in a sequential manner (Doherty et al, 1993), it is increasingly less certain that subsequent CR increments represent the contribution of additional MUs without any instances of alternation.

Many researchers have avoided the problems posed by alternation by studying only the first MU or one MU at a time (Westling et al., 1990; Doherty and Brown, 1994). By taking this approach, these studies have laboriously examined only small numbers (typically one to three) motor units per subject (Chan et al, 1998). Examining the properties of only the first MU in studies using surface stimulation brings about the issue of bias towards low stimulus threshold units. The critical question of whether the

stimulus thresholds of thenar motor axons are in any way related to the physiological properties of their associated motor units is unclear (Chan et al, 1998). Recent research suggests that primarily, the depth of the fiber in the nerve bundle, coupled with axon size (larger axons have lower thresholds) and internal fiber state determine the probability of firing (Szlavik and deBruin, 1999). While these issues remain under investigation, it is widely agreed that the ability to examine the physiological properties of a large sample of MUs per subject is desirable for many reasons, especially those related to diagnosis and monitoring of metabolic neuromuscular disease.

For the purposes of this study, we needed to be confident that every increment in CR was due to the contribution of an additional MU. This being the case, we could then confidently decompose both the CR and ARs into individual MU contributions. This would allow us to study samples of more than a few MUs from each subject and relate our findings to some physiological properties of individual MUs found by other researchers.

It is important to note that for a CR increment to be accepted by our system, it must be encountered repeatedly, a minimum of three times. Such necessity for repeatability is built into the system so that the less probable instances of alternation will be ignored, while the more probable contributions of additional MUs will be accepted as templates. Further, to keep the number of cases of alternation in each study to a minimum, the number of CR increments obtained was kept low. Increments acquired beyond a point of stimulation where multiple examples of alternation were observed in the data were discarded. Finally, an alternation detection algorithm developed by

Cavasin (1989) was used to remove any remaining instances of alternation from the CR records. The algorithm is described in detail by Cavasin (1989), in his thesis. The algorithm requires that each CR template be subtracted from all subsequent ones and any identical solutions are regarded as examples of alternation. While there is a limit to how complicated a case of alternation this algorithm can detect, it works well for CRs with less than fifteen or so increments, where the degree of alternation is confined to a mathematically soluble level.

Since the task for the alternation detection algorithm was minimized to discarding examples of alternation at low-level CR increments, our confidence was assured that the templates retained after the application of the algorithm were due to the contribution of individual MUs. In applying the alternation detection algorithm, only two additional cases of alternation were found and discarded from the low-level CR increments, as shown in Table 4.1.

4.4 EMG Responses

Table 4.1 summarizes the number of EMG and acceleration responses collected during each of the six thenar studies, as well as the number of templates and clean acceleration responses extracted. Up to 17 M-wave templates were obtained for each subject. Excessive motor unit alternation at higher stimulus levels precluded exceeding the number. Figure 3.8 shows the first 6 of 14 CR increments and associated ARs obtained from the left thenar of a 55-year-old male subject in study 2L.

Table 4.1. EMG and Acceleration Responses

	Total # Responses	Filled Templates	Alternation Instances	Motor Unit Templates	Matching Responses	Responses per MU	Clean Abduct.	Clean Flexion	Abduct per MU	Flexion per MU	% Abduct Accepted	% Flexion Accepted
1L	287	9	0	9	163	18.1	138	144	15.3	16.0	84.7%	88.3%
1R	256	17	1	16	204	12.8	118	111	7.4	6.9	57.8%	54.4%
2L	266	14	0	14	161	11.5	81	110	5.8	7.9	50.3%	68.3%
2R	147	12	1	11	76	6.9	42	68	3.8	6.2	55.3%	89.5%
3L	257	17	0	17	231	13.6	143	186	8.4	10.9	61.9%	80.5%
3R	338	11	0	11	180	16.4	56	91	5.1	8.3	31.1%	50.6%
All	1551	80	2	78	1015	13.0	578	710	7.4	9.1	56.9%	70.0%

Assuming linear summation of MUAPs, and that a quantal increase in the M-wave resulted from the addition of one motor unit, the M-wave templates were rank ordered by peak to peak amplitude and successively subtracted to give putative MUAPs. Figure 4.2 (A) shows the putative MUAPs for the first 6 of 14 MUs extracted from the responses shown in Figure 3.8.

4.5 Acceleration Responses

Table 4.1 summarizes the numbers of templates, matching responses and clean abduction and flexion responses recorded in each of the six thenar studies. As outlined in Chapter 3, many acceleration responses were rejected due to excessive noise. 'Clean' acceleration responses were those that exhibited pre-stimulus noise below the threshold level. While the yield of clean responses varied from study to study and with different templates, at least three clean abduction and flexion signals corresponding to each template were recorded and subsequently averaged. For the six thenar studies, the average yield for clean abduction responses was 57% (range 31-85%) and 70% (range 51-90%) for flexion responses.

Analysis of each study's data set showed that the peak-to-peak amplitude of the M-wave templates increased with increasing AR amplitudes as shown in Figure 3.8 and Figure 4.8. Assuming linear summation of MU ARs, and that each increment of the CR resulted from the contribution of an additional motor unit, the ARs corresponding to the rank ordered M-wave templates were successively subtracted to give putative MU ARs. Figure 4.2 (B) shows the putative abduction and flexion MU ARs for the first 6 of 14

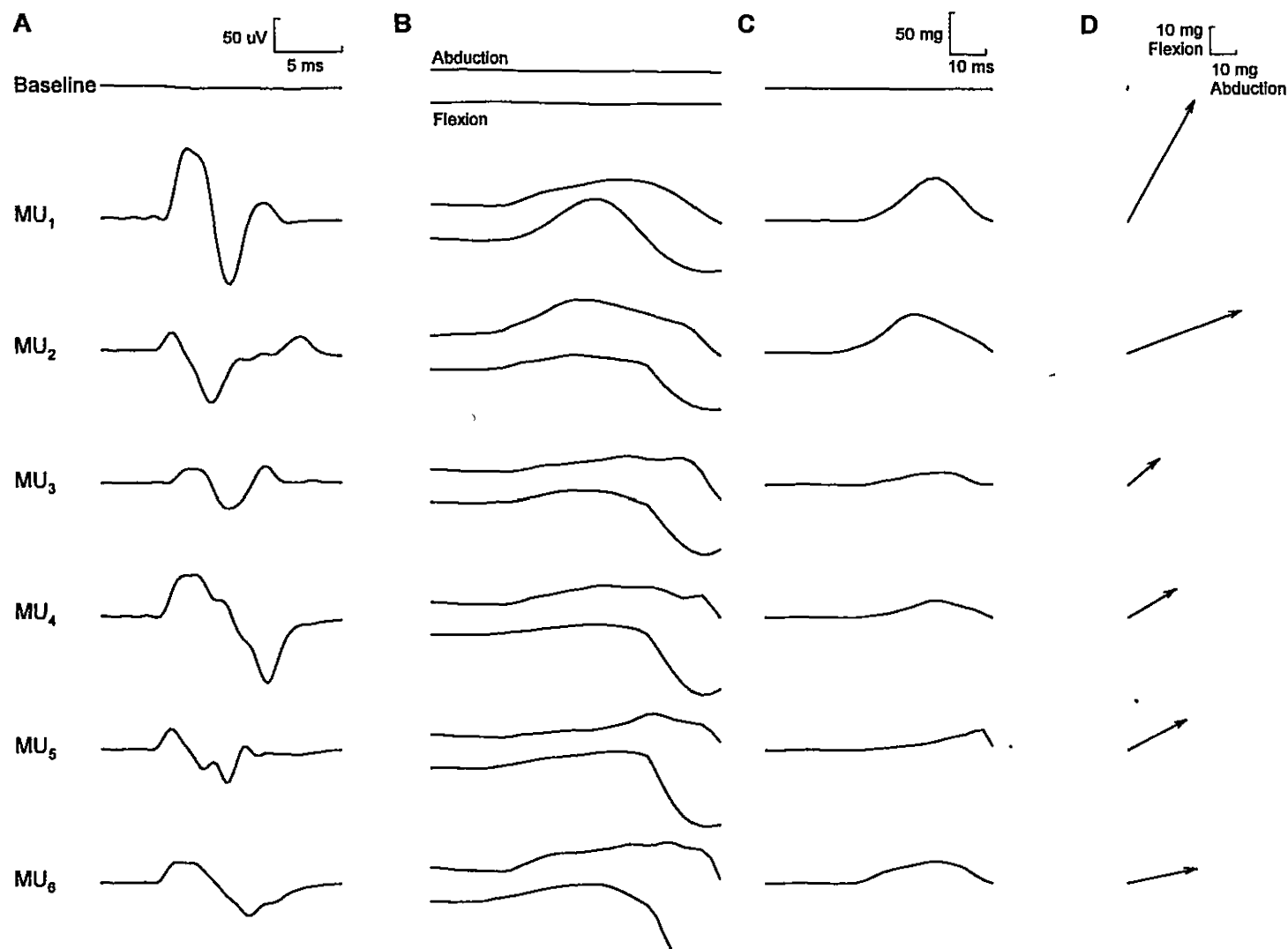


Figure 4.2. Representative extracted MUAPs and their associated acceleration responses.
A: First 6 of 14 extracted MUAPs in study 2L. *B:* associated abduction and flexion acceleration responses.
C: summed acceleration response. *D:* acceleration vector at peak amplitude of summed response.

MUs extracted in study 2L. The abduction and flexion accelerations were squared, summed and the square root taken to produce the composite MU ARs, as shown in Figure 4.2 (C). It was from these composite ARs that peak acceleration amplitude and latency calculations were made. At the time sample corresponding to peak composite acceleration, the abduction and flexion responses were summated to produce the peak acceleration vector for the MU, as shown in Figure 4.2 (D). These vectors indicate the direction and magnitude of peak acceleration produced by each MU.

4.5.1 Smallest Motor Unit Acceleration Responses and Averaging

Although it was initially hoped that the smallest MU ARs could be measured without resorting to signal averaging, through experimentation it was determined that ensemble averaging would be necessary to distinguish the smallest ARs from background noise.

Assuming the noise present in acceleration responses was uncorrelated from signal to signal, all clean ARs associated with a template were ensemble averaged, resulted in substantial signal to noise ratio improvements. Measurable ARs resulted from even the weakest motor units when responses were averaged.

4.5.2 Force and Acceleration

As can be seen from Figure 3.8, the ARs differ considerably from the MU twitch forces recorded by other researchers (Westling et al., 1990; Doherty and Brown, 1994). In their studies the thumb was constrained in a measurement device and only

compressive forces were measured resulting in a monophasic twitch. In contrast, in accelerometry the contraction is not isometric and the tissue elasticity returns the thumb to its original position resulting in the multiphasic acceleration signals shown in Figure 3.8 (B).

The shapes of force and acceleration signals cannot easily be compared. However it can be reasonably assumed that the amplitude of the first peak of the acceleration signal is proportional to the motor unit twitch force. It is also reasonable to assume that peak acceleration latency is proportional to contraction time, which has been measured by other researchers. We therefore used the maximum amplitude of the first positive phase and the latency of this peak to characterize the acceleration response.

4.5.3 Potentiation

At high stimulation frequencies, muscle twitches begin to fuse, increasing their combined strength beyond that achieved by simple summation. In order to avoid such 'staircase' or 'catch' effects (Desmedt and Hainaut, 1968; Burke et al., 1970) associated with stimulation rates above 5 Hz or so, all responses were collected at rates of 1 Hz or less. At these low stimulation frequencies, responses remain separate events (Westling et al., 1990). No evidence of potentiation was observed in any of the present studies.

4.6 Electrical Properties

A summary of electrical properties calculated for the extracted MUAPs is shown in Table 4.2. Negative peak areas are shown in favour of total area under the curve to facilitate comparison with data from other studies.

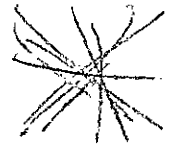


Table 4.2. Electrical Properties of Motor Units.

	MUs	Peak to Peak (μV)			-ve Area ($\mu\text{V}\cdot\text{ms}$)			MUAP Latency (ms)		
		Mean	Std Dev	Median	Mean	Std Dev	Median	Mean	Std Dev	Median
1L	9	114	92	126	228	177	230	7.5	0.7	7.4
1R	16	76	128	33	133	190	80	8.7	1.5	8.5
2L	14	48	47	41	59	92	46	6.6	0.9	6.8
2R	11	65	67	45	103	107	88	5.2	0.6	5.3
3L	17	83	149	59	158	299	89	6.5	1.5	6.1
3R	11	41	76	17	71	134	32	7.1	1.3	6.9
All	78	70	104	40	123	192	83	7.0	1.6	6.8

4.6.1 MUAP Peak to Peak and Area

As illustrated in the histograms of Figure 4.3, the 78 extracted MUAPs ranged in size from less than 10 μV to 650 μV peak to peak amplitude (B) and from less than 20 $\mu\text{V}\cdot\text{ms}$ to 1300 $\mu\text{V}\cdot\text{ms}$ in negative peak area (A). As found in other studies, these distributions were skewed towards smaller units. The average MUAP peak to peak amplitude was 70 μV , while the average negative area was 123 $\mu\text{V}\cdot\text{ms}$. Both distributions demonstrate a wide range indicating that a variety of MU sizes were sampled.

In comparison, a study of 200 units extracted from 10 subjects by Stein and Yang (1990) using the McComas technique resulted in a similar MUAP peak to peak amplitude range of less than 10 μV to 1000 μV , with an average peak to peak amplitude of 102 μV .

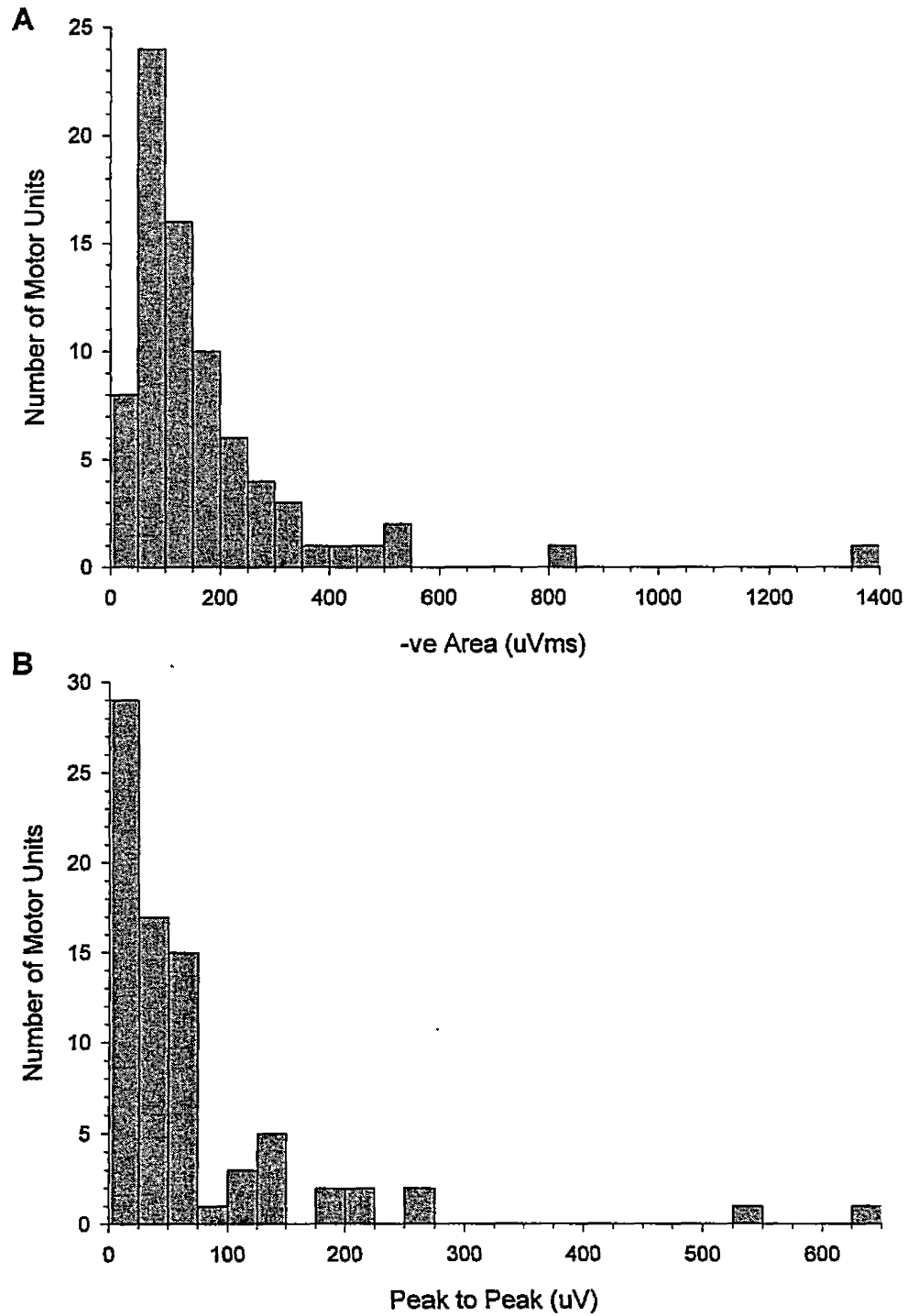
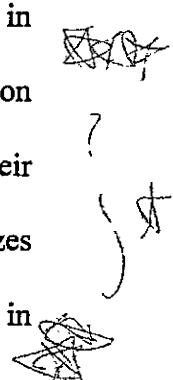


Figure 4.3. Distribution of thenar MUAP sizes. *A*: -ve area. *B*: peak to peak amplitude.

Stein and Yang noted that when considering the average MUAP size elicited using spike triggered averaging and intramuscular microstimulation, it is necessary to consider the composite single unit time course for both the EMG and force measures. When MUAPs sampled with the microstimulation method were aligned and summated, average unit size was approximately 28% smaller than the original value determined by the simple average of single unit sizes. The resulting average MUAP peak to peak amplitude of 87 μ V is similar to that found in the present study.

Using multiple point stimulation and surface recording of 380 units from subjects with ages ranging from 19 to 38, Doherty and Brown (1993) found a peak to peak surface recorded MUAP amplitude range of 5 to 1042 μ V, with a mean (\pm SD) of 87 (\pm 96) μ V, and median of 61 μ V. MUAP negative area ranged from less than 10 to 2250 μ V \cdot ms with a mean (\pm SD) of 157 (\pm 206) μ V \cdot ms and median of 98 μ V \cdot ms. These MUAP size distributions agree well with those of Stein and Yang (1990) and the present study.

Differences in parameters between studies may be attributed to differences in recording electrode configurations, which significantly influence amplitude and duration of surface recorded MUAPs. Examining the distributions of parameters over their respective ranges, it would appear from comparison with the above studies that the sizes of the MUs sampled in the present study are reasonably representative of those found in larger MU populations.



4.6.2 MUAP Latency

MUAP peak latencies in the present study demonstrated a wide range (4.8 to 11.5 ms) with a mean (\pm SD) of 7.0 (\pm 1.6) ms and a median of 6.8 ms. This range and distribution, as shown in Figure 4.4, agrees well with the calculated latencies of the large pool of 380 units examined by Doherty and Brown (1993). They found a wide range (5.2–11.8 ms) in the adjusted latencies of the surface MUAPs collected by multiple point stimulation, with a mean adjusted latency of 6.7 ± 1.0 ms. This distribution was similarly skewed toward shorter latencies with a median value of 6.5 ms.

4.7 Contractile Properties

A summary of contractile properties calculated for the extracted MU ARs is shown in Table 4.3. Peak acceleration was determined from the composite AR. The units sampled were not obviously biased in favour of units that produce weak or strong forces. Data from individual subjects included units producing both small and large accelerations, with contractile forces and rates spanning the range of the total population.

Table 4.3. Contractile Properties of Motor Units

	MUs	Peak Acceleration (mg)			Acceleration Latency (ms)			Peak Acceleration Angle (degrees)		
		Mean	Std		Mean	Std		Mean	Std	
			Dev	Median		Dev	Median		Dev	Median
1L	9	18.6	18.5	15.9	32.5	4.5	31.0	72.5	25.8	85.9
1R	16	3.5	1.9	2.8	29.3	4.5	30.0	62.2	37.7	64.8
2L	14	24.5	14.9	22.2	41.8	5.7	42.0	27.0	28.8	27.6
2R	11	7.1	6.1	6.4	32.6	3.5	0.0	41.0	37.0	39.2
3L	17	5.0	7.8	2.4	30.9	6.4	33.0	41.2	49.3	23.4
3R	11	23.3	36.0	9.1	31.6	6.4	32.0	55.5	34.5	48.4
All	78	12.6	18.4	4.8	33.1	6.7	32.0	48.5	39.3	44.3

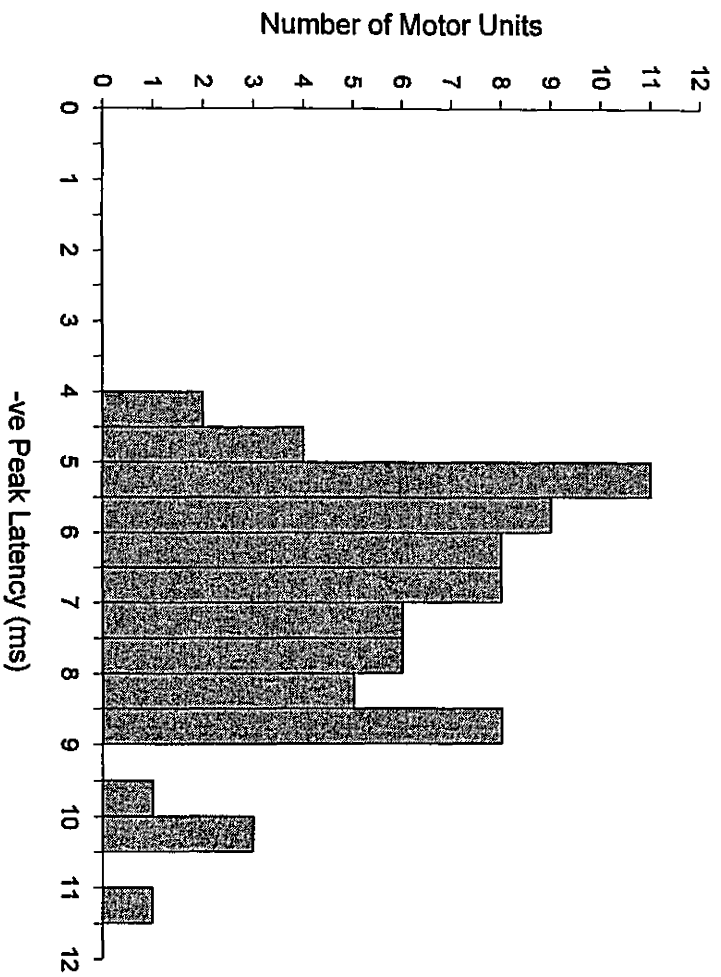


Figure 4.4. Distribution of thenar motor unit peak latencies.

4.7.1 Peak Acceleration Magnitude and Direction

Abduction and flexion components of acceleration can be analyzed individually to determine the magnitude and direction of peak acceleration for each motor unit, as has been done by other researchers measuring twitch forces. Thomas et al. (1990) found that individual motor units within the same muscle group generate force in widely different directions. The present study supports these findings. Acceleration responses measured in two directions were found to vary widely with respect to their primary vector. Had acceleration been measured in only one direction (eg., abduction) as done by Stein and Yang (1990), the acceleration distributions would have been biased toward lower values. Several strong units, which produced most or all of their acceleration in the flexion direction would have registered only small accelerations, or their acceleration outputs would have been missed completely (Thomas et al., 1990). It is therefore important that a two-axis collection system be used when studying muscles acting in two dimensions. Figure 4.5 shows the peak acceleration vectors of all 78 MUs studied.

Peak acceleration magnitude for all 78 MUs ranged from 0.25 to 125 mg, with a positively skewed distribution, as shown in the histogram of Figure 4.6 (A). The acceleration of >50% of units was <6 mg. Thomas et al. (1990), found that in a sample of 45 units, twitch forces ranged from 2.9 to 34.0 mN, with >50% of units exerting force of <10 mN. While it is difficult to compare absolute acceleration and force measurements due to the unknown interaction of limb mass and joint dynamics, it is reasonable to assume that they are directly proportional. In this light, it is reasonable that

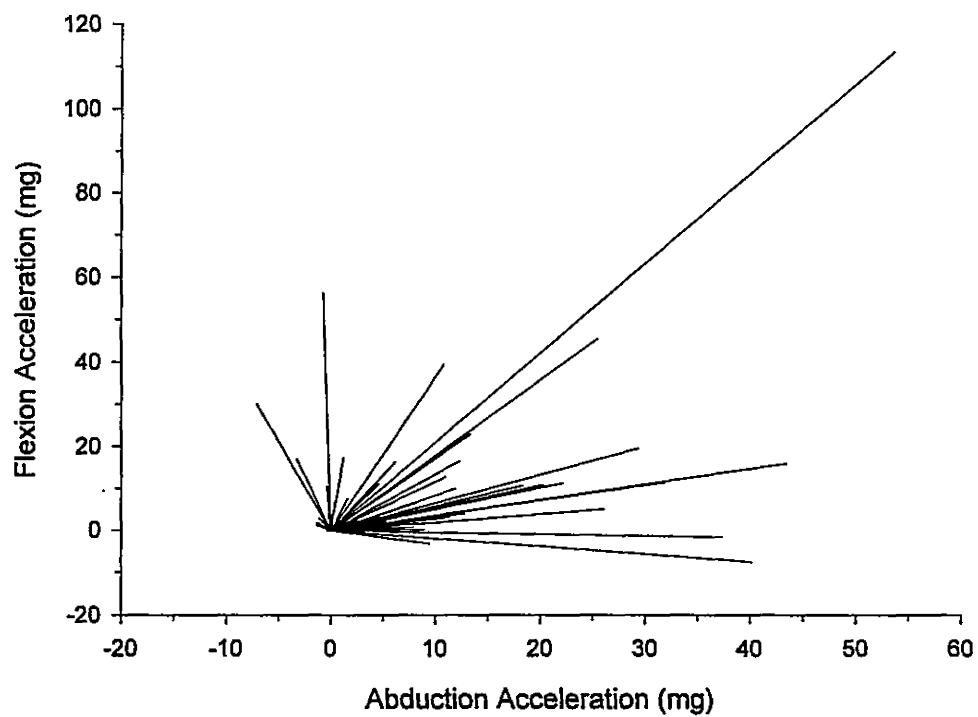


Figure 4.5. Peak Motor Unit Acceleration Vectors.

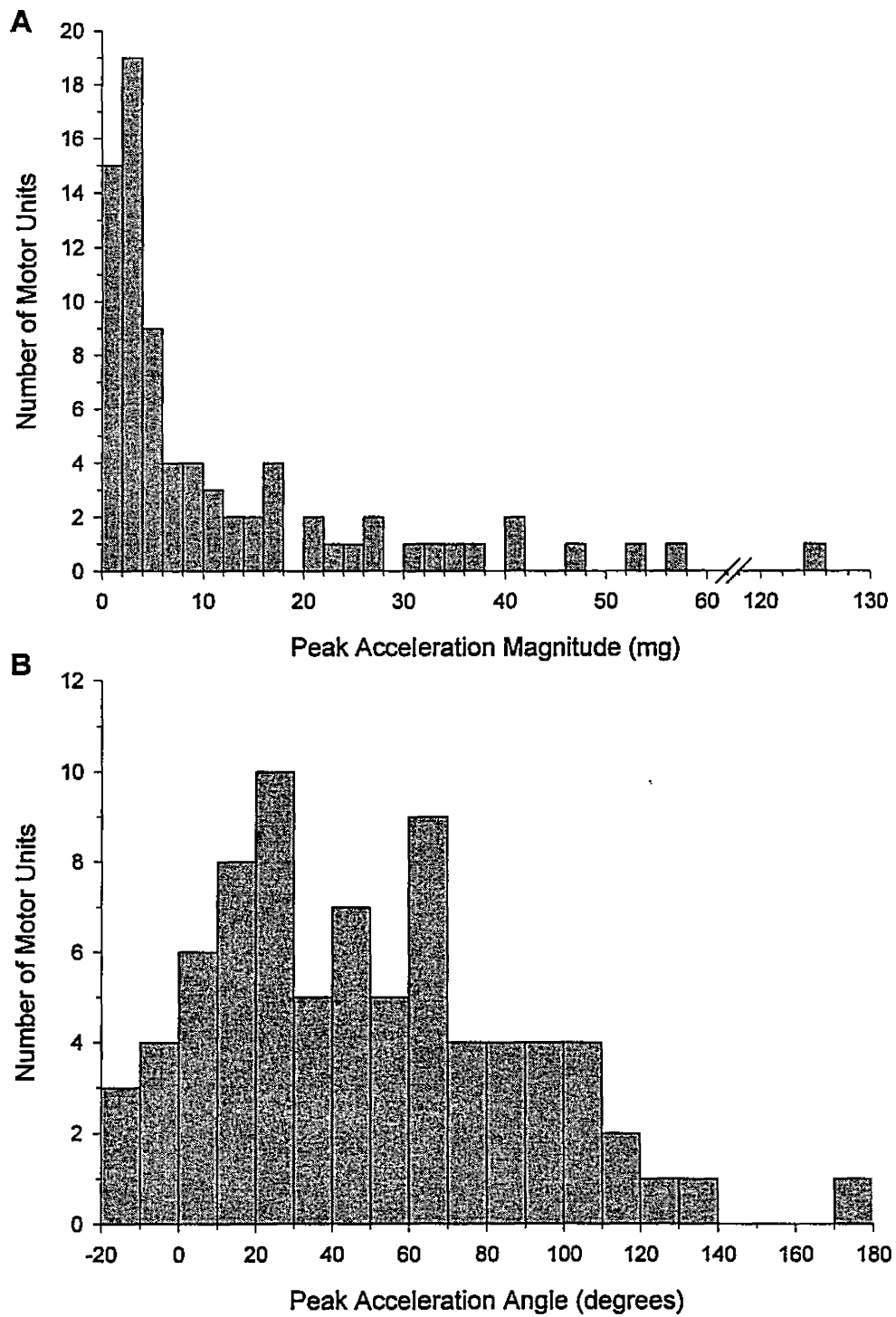



Figure 4.6. Distribution of thenar motor unit peak acceleration responses.
A: magnitude. *B*: direction.

the distributions outlined above should agree in their skew towards small force and acceleration units.

Most units (86%) studied by Thomas et al. exerted force between 0 and 90° (referring to abduction and flexion, respectively) with an overall range of -47 to 124°. Similarly, the angles of peak acceleration for the 78 MUs in the present study ranged from -18 to 135°, with most units (80%) falling between 0 and 90°, as shown in Figure 4.5.

Also agreeing with the findings of Thomas et al., in the present study there was no obvious relationship between magnitude and angle of acceleration. Nor was there any grouping of acceleration vectors, as would indicate that units were sampled from separate muscles within the thenar group. 

4.7.2 Peak Acceleration Latency

Peak acceleration latencies can be calculated for each motor unit and compared to the contraction times and contractile rates derived from twitch forces in other studies. Obviously, fast twitch motor units should have faster acceleration times than slow twitch units. As shown for typical putative ARs in Figure 4.2 (C), inspection of composite acceleration response data showed considerable variation in the peak latency of the first positive phase of the acceleration. The peak latencies presented in this study span a range of 18-50 ms, with a reasonably normal distribution as shown in Figure 4.7.

Joint dynamics make direct comparisons between peak acceleration latency and twitch contraction time difficult. Thomas et al. (1990), presented measurements of

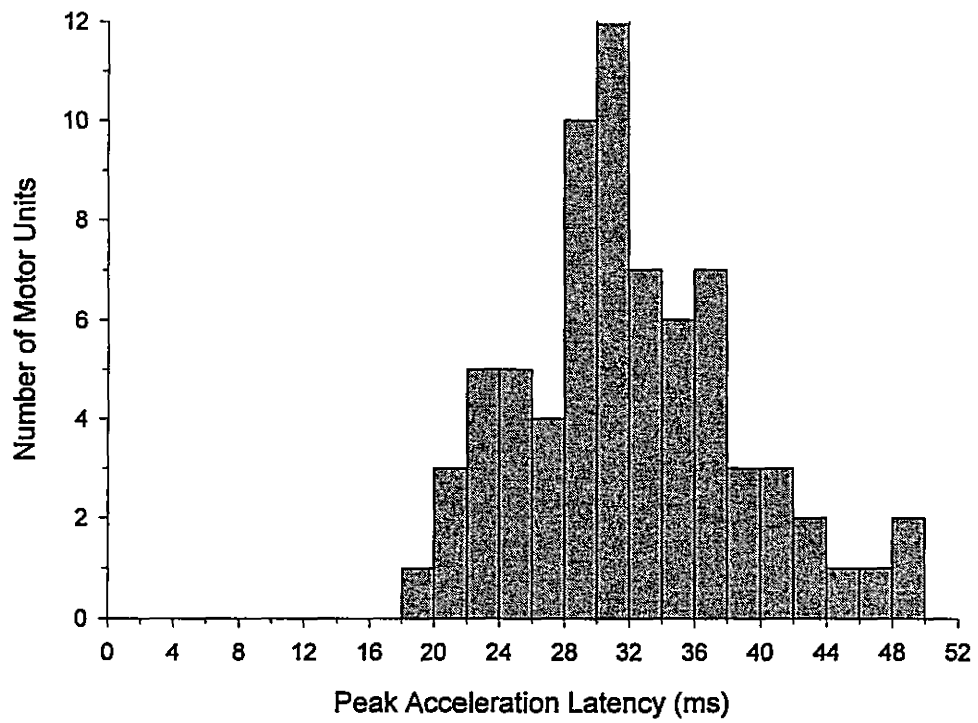


Figure 4.7. Distribution of thenar motor unit peak acceleration latency.

contraction time ranging from 35-80 ms for 45 thenar motor units, while Doherty and Brown (1997) reported a range of 28-93 ms for 92 MUs of younger and older subjects combined.

The time to peak acceleration for a free to move limb is shorter than the time to peak isometric force. This is because the muscle is shortening as peak force is produced. A study by Gravel et al. (1987) showed that when human plantarflexor muscles are stimulated during passive shortening, contraction time decreases and relaxation time increases. The peak force production during passive shortening was decreased but was just as stable and repeatable as peak force during static conditions or passive lengthening. The fact that the thenar is shortening does not affect the proportionality of the peak acceleration to the peak muscular force produced. Tendon elasticity was considered to be negligible at the force levels considered.

The acceleration signal is a multiphasic signal, which becomes negative even before the limb has reached its full range of forward motion. Isometric force measured by strain gauge is a monophasic signal, which builds from zero, peaks, and returns to zero. It is intuitive that force output measured by strain gauge would continue to rise for at least the duration of the first positive phase of acceleration. While extremely difficult to demonstrate, it is therefore reasonable that contraction time should lag peak acceleration latency.

In light of these comments, the ranges presented above seem reasonable. Contraction time ranges in the two studies cited are slightly less than double the peak acceleration latency range found in the present study, while the distribution of the present

study agrees well in shape and skew with the distributions of contraction times reported by Thomas et al. (1990) and Doherty and Brown (1997).

Being able to determine the percentage of slow and fast twitch fibers and hence motor units would be of great value especially in the diagnosis and monitoring of metabolic neuromuscular disease. It would appear, however, that in the absence of a bimodal or multimodal distribution, the MUs sampled may not be easily divided into fast and slow types based on differences in their peak acceleration latencies. This lack of obvious bimodal or multimodal distribution in contractile rate is in agreement with the findings of Thomas et al. (1990) and Doherty and Brown (1997). Thomas et al. (1990) went further to find that none of the conventional measurements of twitch contraction time, force ratio, or 'sag' clearly separate human thenar units into distinct groups of fast or slow types.

4.8 Relationships Between Parameters

As shown in Table 4.4, MU peak acceleration amplitude was significantly correlated with MUAP peak to peak amplitude and MUAP area. Correlation was strong in data from individual subjects, especially in data from studies 3L and 3R, due in part, however, to large MUAP and acceleration magnitude contributions made by a single unit in each study.

Table 4.4. Correlation coefficients between parameters.

Correlation ($p < .05$) of Peak Acceleration with:				
	MUAP Pk-Pk	MUAP -ve Area	MUAP Latency	Accel. Latency
1L	0.63	0.61	-0.46	0.44
1R	0.33	0.47	0.26	0.45
2L	0.62	0.32	0.00	-0.15
2R	0.68	0.80	0.02	-0.46
3L	0.91	0.91	-0.07	-0.05
3R	0.95	0.94	0.34	0.21

The amplitude of a motor unit potential is affected by the position of that unit within the muscle belly; the more deeply a motor unit is situated, the smaller the potential projected to the recording electrodes on the overlying skin (Szlavik and deBruin, 1999). However, the position of a MU within the muscle belly would not likely affect the force or acceleration produced by that unit in the same manner, and correlation between MUAP size and peak acceleration would therefore be weakened. }

Although individually, each subject presented examples of small and large MUs virtually spanning the range for the entire population, due to variation in subject and recording configuration, it was felt that the pooling of data would provide an inadequate calculation of global average correlation.

As might be expected, no significant correlation was found between acceleration magnitude and MUAP latency. Also, no significant correlation was found between MUAP peak to peak magnitude or area and peak acceleration latency.

Correlation between acceleration magnitude and acceleration peak latency was weak for the entire population as well as for data obtained from individual subjects. Researchers examining force and contraction time in other human studies have found weak or absent correlation as well.

This is in contrast to animal studies, where twitch forces are generally reported to be inversely related to contraction times (Thomas et al., 1990). As Thomas et al. point out, and Rafuse et al. (1997) support, in cat and rat muscles, the fibers of the faster, stronger units (fast fatigable) are about twice the diameter of those of the weaker (slow) units, and the number of fibers per MU (innervation ratio) is larger for fast fatiguing than for slow units. This wide range in innervation ratios can account for the inverse correlation between force and contraction time found in animals. } *

In man, however, no such differences have been established and no consistent difference between type I and II fiber diameters has been found. Thus, although the findings of weak correlation between acceleration magnitude and latency are at odds with animal studies, they are in agreement with recent human studies (Thomas et al., 1990; Doherty and Brown, 1997).

4.9 Motor Unit Number Estimation

The original purpose of the McComas technique was to provide a method of calculating a motor unit number estimate (MUNE) for a given subject. Several studies have provided MUNE's based on MUAP feature extrapolation using various techniques discussed below, however, few MUNE's have been made using the contractile properties of MUs (see however, Stein and Yang, 1990; Eleveld, 1992).

In addition to conventional MUNE's based on MUAP feature extrapolation, in the present study, maximum and single unit ARs were used to obtain independent MUNE's based on acceleration measurements. Summaries of MUNE calculations by MUAP and

peak acceleration extrapolation for each of the six thenar studies are presented in Table 4.5.

4.9.1 MUAP Extrapolation

As described in Chapter 2, by dividing the amplitude of the largest response in the CR by the number of increments, an estimate of the average MUAP amplitude contribution for the thenar is obtained. Further, by dividing the amplitude of the MEP by the average MUAP amplitude contribution, one obtains an estimate of the number of MUs in the muscle. The McComas technique is a fast and noninvasive MUNE method.

The main criticism of this technique has been the possibility that the size of the average MUAP is underestimated due to an excessive number of CR increments resulting from alternation. To avoid the problems posed by alternation, other more indirect methods of collecting a sample of single MUAPs from which the average MUAP size may be calculated have been developed. These include multiple point stimulation (Doherty and Brown, 1993), spike-triggered averaging (Brown et al., 1988) and microstimulation (Stein and Yang, 1990). However, since these methods are applied at multiple sites, the temporal relationships between the latencies and phases of the individual MUAPs, which are naturally incorporated within the MEP, are lost (Doherty and Brown, 1993). This can lead to an overestimation of the average MUAP size, since the cancellation which normally occurs between opposite phases of summated MUs is absent when single MUAPs are recorded at different sites. While the error may be minimized by setting the latencies of all MUAPs to zero and then averaging the

Table 4.5. Motor Unit Number Estimates by M-Wave and Peak Acceleration Extrapolation.

	Number of Templates	M-Wave Area Extrapolation				Peak Acceleration Extrapolation			
		Largest Tmp. Area (uV.ms)	Average Tmp. Area (uV.ms)	MEP Area (uV.ms)	MUNE	Largest Tmp. Peak (mg)	Average Tmp. Peak (mg)	MEP Peak (mg)	MUNE
1L	9	3.96	0.44	42.9	98	132	14.6	692	47
1R	16	4.54	0.28	37.9	133	35	2.2	548	248
2L	14	2.17	0.16	54.7	352	314	22.4	1235	55
2R	11	1.79	0.16	29.5	181	61	5.6	174	31
3L	17	5.22	0.31	34.2	111	58	3.4	975	287
3R	11	1.25	0.11	35.8	314	223	20.3	1242	61
All	13	3.15	0.24	39.1	198	137	11.4	811	122
Std. Dev.	3	1.63	0.12	8.8	109	110	8.9	420	114

waveforms datapoint by datapoint, there is no agreed upon method to determine whether the resulting average is an accurate representation of the MU population.

One of the key advantages of using the McComas method, is that these latency and phase relationships are naturally preserved because the average MUAP size is determined from a compound potential evoked by stimulating the nerve at the same site as used for the MEP. The McComas technique is also the most rapid and least invasive technique (Stein and Yang, 1990), and since recording is performed at the same site in a continuous session, changes in MUAP records due to subject and electrode movement are minimized.

For the six thenar studies presented in this thesis, the mean (\pm SD) MUNE calculated by MUAP area extrapolation was $198 (\pm 109)$. Although based on only six subjects, this value is in agreement with several recent studies using different techniques, as shown in Table 4.6.

Table 4.6. Summary of Thenar Motor Unit Number Estimates from Recent Studies.

Methods	MUNE (Mean \pm SD)	Investigator
MUAP extraction methods:		
Automated McComas	228 ± 93	Galea et al., 1991
Multiple Point Stimulation, Pk-Pk	206 ± 58	Doherty and Brown, 1993
-ve Area	288 ± 95	Doherty and Brown, 1993
Spike-Triggered Averaging	135 ± 27	Stein and Yang, 1990
Microstimulation	122 ± 38	Stein and Yang, 1990
Manual Incremental McComas	170 ± 62	Stein and Yang, 1990
Automated McComas	198 ± 109	Orsi (current study)
Force / Acceleration methods:		
Spike-Triggered Averaging, Force	130 ± 39	Stein and Yang, 1990
Microstimulation, Force	135 ± 45	Stein and Yang, 1990
Automated McComas, Accel.	122 ± 114	Orsi (current study)

4.9.2 MU Peak Acceleration / Force Extrapolation

As done for MUAP extrapolation, the amplitude of the AR corresponding to the largest response in the CR can be divided by the number of CR increments, to obtain an estimate of the average MU AR amplitude for the thenar. Then, by dividing the amplitude of the MEP's AR by the average MU AR amplitude, one obtains an estimate of the number of MUs in the muscle.

Using average thenar MU force and maximum thenar force, Stein and Yang (1990) calculated MUNE's based on responses collected from both spike-triggered averaging and microstimulation, as shown in Table 4.6.

For the six thenar studies presented in this thesis, the mean (\pm SD) MUNE calculated by MU AR amplitude extrapolation was 122 (\pm 114). Although based on only six subjects, this value is in agreement with the force studies of Stein and Yang (1990), as shown in Table 4.6.

Stein and Yang (1990) found good agreement between MUNE's based on MUAP extrapolation and force extrapolation. However, as shown in Table 4.5, for the individual thenars examined in the present study agreement between MUAP extrapolation and MU AR amplitude extrapolation was quite poor in several cases.

4.9.3 Implications

Ultimately, the solution to achieving more accurate MUNE's lies in sampling a larger number of MUs from a given population. A larger sample is more likely to exhibit a distribution characteristic of the entire MU population.

Unfortunately, when using the incremental stimulation technique, complications such as alternation introduce barriers to decomposing CRs of more than 20 MUs. No clear method exists to accurately determine the number and characteristics of MUs decomposed from CRs with such high numbers of increments. Thus, useful samples are limited to approximately the first 10% of MUs contributing to the MEP. If these first few MUs do not exhibit distributions characteristic of the entire MU population, MUNE will err significantly.

Figure 4.8 shows the results of graded whole nerve stimulation for four of the six thenar studies. Graded stimulation was not performed in the other two thenar studies due to time constraints. The relationship between M-wave peak to peak amplitude and peak acceleration is shown, for sub-threshold to MEP stimulation levels. Measurements for the collected templates of the four studies are superimposed to illustrate the characteristics of the sample with which MUNE were extrapolated. Given the variety in initial slopes shown in Figure 4.8, the assumption that the small sample studied is representative of the entire MU population may not be accurate. However, other systems, which base MUNE on even smaller numbers of MUs per subject may be even less accurate in their representation of the average member of the overall population.

With such disparate results between MUAP and MU AR amplitude extrapolation for individual subjects, as shown in Table 4.5, the question of which method is more reliable must be examined. The coefficients of variation for both techniques may be determined using multiple site stimulation. Assuming that the lowest threshold units vary with point of stimulation along the median nerve, different sets of MUs from the same

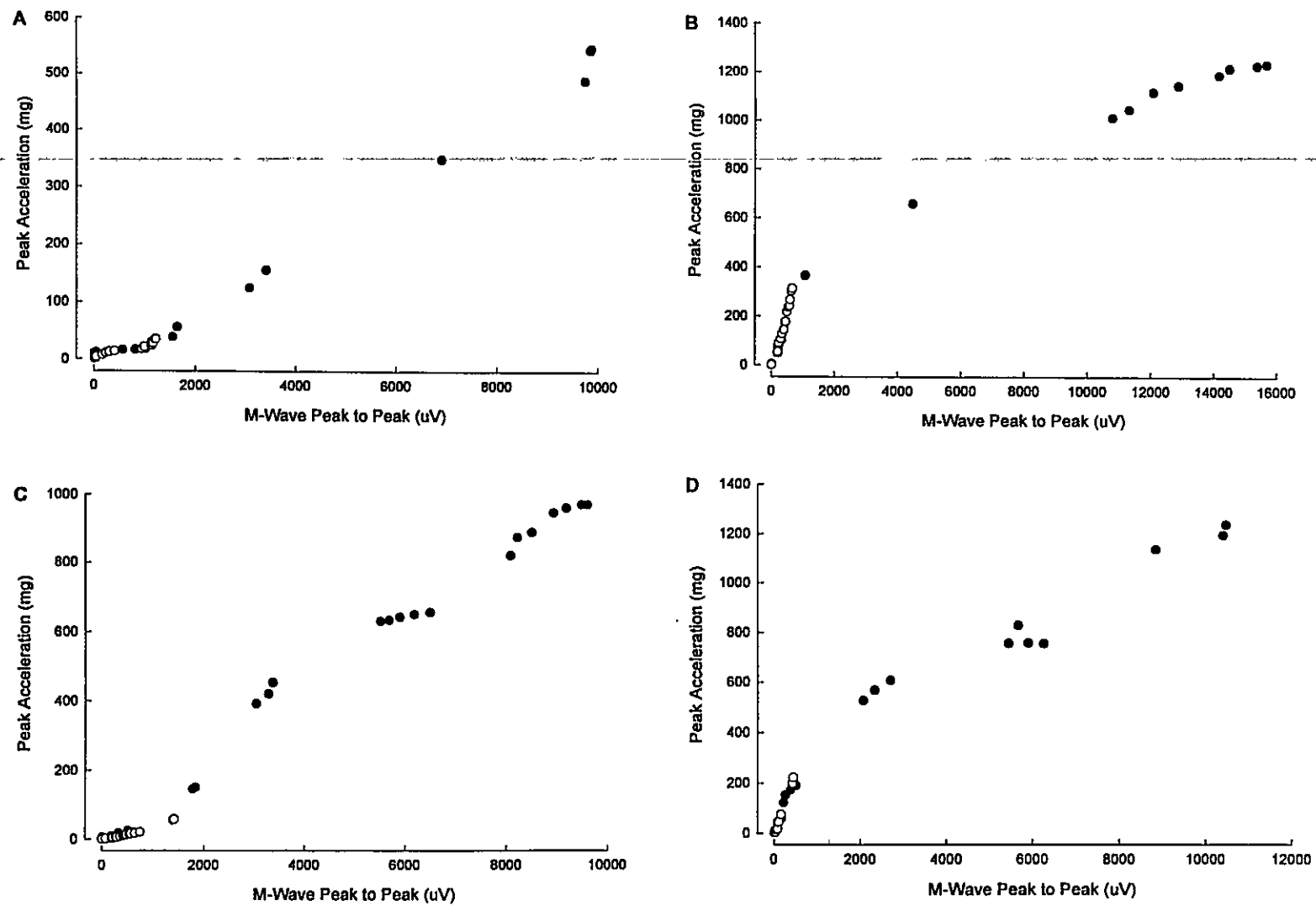


Figure 4.8. Peak to Peak vs Peak Acceleration for Templates (O) and Graded Responses (●) in Studies 1R(A), 2L(B), 3L(C), and 3R(D).

population may be excited and examined by performing template collections at multiple stimulation sites. The technique demonstrating the smallest coefficient of variation should prove to be the most reliable extrapolation technique. However, some uncertainty will always exist when extrapolating MUNEs from a small subset of the overall MU population.

CHAPTER 5

EMG PATTERN RECOGNITION TECHNIQUES

5.1 EMG Pattern Recognition

Historically, grouping composite responses created by distinct sets of MUs has gone from visual inspection to automatic classification done by computer. The human mind is extremely adept at discriminating action potentials and is capable of accurate and repeatable classification. However, with increased computing power and innovative use of signal processing tools such as Fourier and wavelet analysis, automated techniques enjoy greater and greater efficiencies over human visual recognition.

Whether the classification is done visually or automatically it follows the same general pattern recognition scheme:

- 1) Extraction of features of the signal that are known to be significant in separating one group of signals from another.
- 2) Assembly of the numeric values of the selected features into regions occupied by the different groups based on the feature vectors of known samples from each group, or a priori knowledge.
- 3) Classification of a new signal based on the region in feature space in which its vector is located (Duda and Hart, 1973).

In the automated classification of M-waves into templates, the process of feature selection is the single most important step, since it determines both the speed at which the

classification can be accomplished and the accuracy and repeatability of the classification procedure. Optimally, the ideal set of features describing the CR increments would be as statistically independent as possible in order to successfully classify all of the M-waves that could be encountered in any particular study.

While time domain feature comparison is a viable option that has been used extensively in the past, frequency domain Fourier analysis and time-scale domain wavelet analysis offer certain advantages in making clearer distinctions between templates or groups. This chapter attempts to explain the basic principals of time, Fourier and wavelet analysis techniques when applied to the problem of EMG pattern recognition. A comparative study of the effectiveness of the techniques is also presented, using real signals and their extracted features from the six thenar studies presented in Chapter 4.

5.1.1 Latency Shifting

Electrical stimulation of an AP in the motor axon is most likely to occur at the nodes of Ranvier (see Figure 2.1). Depending on the current distribution under the stimulating electrodes, initiation of the AP will occur simultaneously at several nodes close to the cathodic electrode. Stimulation of the most distal node determines the latency of the resulting MUAP. If the most distal of these nodes is just on the threshold of activation, on repeated stimulation, the site of AP initiation may alternate between this node and the next most proximal node. Such a shift in the AP initiation site will cause a discrete shift in the response latency corresponding to the time required to traverse the

internodal distance. Small displacements of the stimulating electrodes during a test will cause similar changes in response latency.

As noted by Cavasin (1989) and others, this phenomenon has important implications for pattern recognition of EMG signals. A manual operator would be able to recognize and ignore a small discrete latency shift, due to his or her concentration on the more crucial shape and size of each response. However, two M-waves identical in shape and size may be mistaken for different responses by an automated pattern recognition technique that compares signals based on their alignment in time. This potential drawback of time-based EMG pattern recognition must be kept in mind when evaluating techniques.

5.2 Frequency Domain Classification

Fourier analysis breaks down a signal into constituent sinusoids of different frequencies. It is a mathematical technique for transforming the signal from a time-based representation to a frequency-based one. Fourier analysis is extremely useful when applied to an EMG response because the signal's frequency content can be thought of as a fingerprint, which can be used to match the signal to, or distinguish it from, other responses.

Mathematically, the process of Fourier analysis is represented by the Fourier transform:

$$F(\omega) = \int_{-\infty}^{\infty} f(t) e^{-j\omega t} dt \quad 5.1$$

which is the sum over all time of the signal $f(t)$ multiplied by a complex exponential. The results of the transform are the Fourier coefficients $F(\omega)$, which describe the constituent sinusoidal components of the original signal.

Since computation of Fourier series coefficients and Fourier transform requires integration, the function must be describable analytically by elementary functions such as sine and cosine functions, exponential functions and terms from a power series. In general, most signals we encounter in real life cannot be represented by elementary functions. We must use numerical algorithms to compute the spectrum. If the signals are sampled signals, such as those of the present study, the discrete Fourier series and discrete-time Fourier transform (DFT) are computable directly. They produce an approximate spectrum of the original analog signal. We can obtain a good approximation by a discretization on the frequency (ω) axis. Since the function $f(t)$ is bandlimited (if it is not, we make it so by passing it through a lowpass filter with sufficiently large width), we need to discretize the interval $[-\Omega, \Omega]$ only, where namely:

$$\omega_n = \frac{2\pi n}{Nh}, \quad n = -\frac{N}{2}, \dots, \frac{N}{2}$$

where N is the number of data samples (128 in our case), h is the sampling period (.250 ms in our case) and Ω is the sampling frequency (4 kHz in our case). The Fourier transform integral can now be approximated as a series sum, namely:

$$F(\omega_n) \approx h \sum_{k=0}^{N-1} f(kh) e^{-j\omega_n kh} = h F(n), \quad 5.2$$

where

$$F(n) = \sum_{k=0}^{N-1} f(kh) e^{-j(2\pi kn/N)} \quad 5.3$$

We can easily verify that evaluation of the discrete Fourier transform is an $O(N^2)$ process. We can, however, compute the DFT much more efficiently with an $O(N \log_2 N)$ operation by using the well-known algorithm of the fast Fourier transform (FFT). According to the commonly used Danielson and Lanczos FFT algorithm, assuming N to be continuously divisible by 2, a DFT of data length N can be written as a sum of two discrete Fourier transforms, each of length $N/2$. This process can be used recursively until we arrive at the DFT of only two data points. This is known as the radix-2 FFT algorithm (Goswami and Chan, 1999). In summary, by appropriately arranging the data of length N , where N is an integer power of 2 (known as decimation-in-time arrangement), we can compute the discrete Fourier transform in an $O(N \log_2 N)$ operation. If N is not an integer power of 2, we can always make it so by padding the data sequence with zeros. Normally, the data sequence is multiplied by a shaping window such as Hamming (Proakis and Manolakis, 1995) to ensure that the initial and final samples of the data sequence smoothly approach zero. This was not necessary for M-wave analysis because the initial and terminal amplitude of the M-waves are already zero as shown in Figure 3.3 (B). In the present study, zeros are added to ends of the M-wave data window, as shown in Figure 3.7 (C) to provide 128 data samples for the FFT algorithm. The magnitudes of the 2nd through 21st emerging coefficients are used as features to discriminate between signals. By taking only the magnitude spectrum of these coefficients, phase information is discarded.

An important characteristic of Fourier analysis is that in transforming to the frequency domain, time information is lost. When looking at a Fourier transform of a signal, it is impossible to tell when a particular event took place. If a signal is stationary, or if frequency information alone is sufficient, this potential drawback is not important. However, if a signal contains numerous non-stationary or transitory characteristics such as drift, trends, or abrupt changes, which are important parts of the signal, Fourier analysis may not be suitable.

5.3 Short-Time Fourier Analysis

In an effort to conserve both time and frequency information in signal analysis, Gabor (1946) adapted the Fourier transform to analyze only a small segment of the signal at a time by windowing the signal. Gabor's adaptation, called the Short-Time Fourier Transform (STFT), maps a signal into a two-dimensional function of time and frequency. The software presented in this thesis calculates and displays a contour mapping of STFT coefficients in the upper left corner of the GUI, as shown in Figure 3.3 (A).

The STFT represents a compromise between the time- and frequency-based views of a signal. It provides some information about both when, and at what frequencies, a signal event occurs. However, this information can only be obtained with limited precision, which is determined by the size of the window.

While the STFT's compromise between time and frequency information can be useful, the drawback is that once a particular window size is chosen, that window is the same for all frequencies. A tradeoff between time and frequency resolution is made. A

more desirable approach – one where the window size can be varied to determine with more accuracy either time or frequency – is presented by wavelet analysis. For this reason, other than calculating and displaying a contour map of the STFT coefficients on the GUI for reference, further use and study of the STFT was not pursued and is beyond the scope of this thesis.

5.4 Wavelet Based Classification

Wavelet analysis represents a windowing technique with variable-sized durations. Long time intervals are used where more precise time information is needed, and shorter segments are used where more precise frequency information is needed. Wavelet analysis can be used to analyze a localized segment of a larger signal, revealing aspects of data that Fourier analysis may miss - aspects such as trends, breakdown points, discontinuities in higher derivatives, and self-similarity.

A wavelet is a waveform of limited duration that has an average value of zero. In comparison, Fourier analysis is based on sine waves, which do not have limited duration, extending from minus to plus infinity. Where sinusoids are smooth and predictable, wavelets tend to be irregular and asymmetric, as shown in Figure 5.1 (B).

Fourier analysis consists of decomposing a signal into sine waves of various frequencies. Similarly, wavelet analysis is the decomposition of a signal into shifted and scaled versions of the original (or mother) wavelet.

It is intuitive that complex transient signals might be better analyzed with an irregular wavelet than a smooth sinusoid. For the purposes of this study, we used the

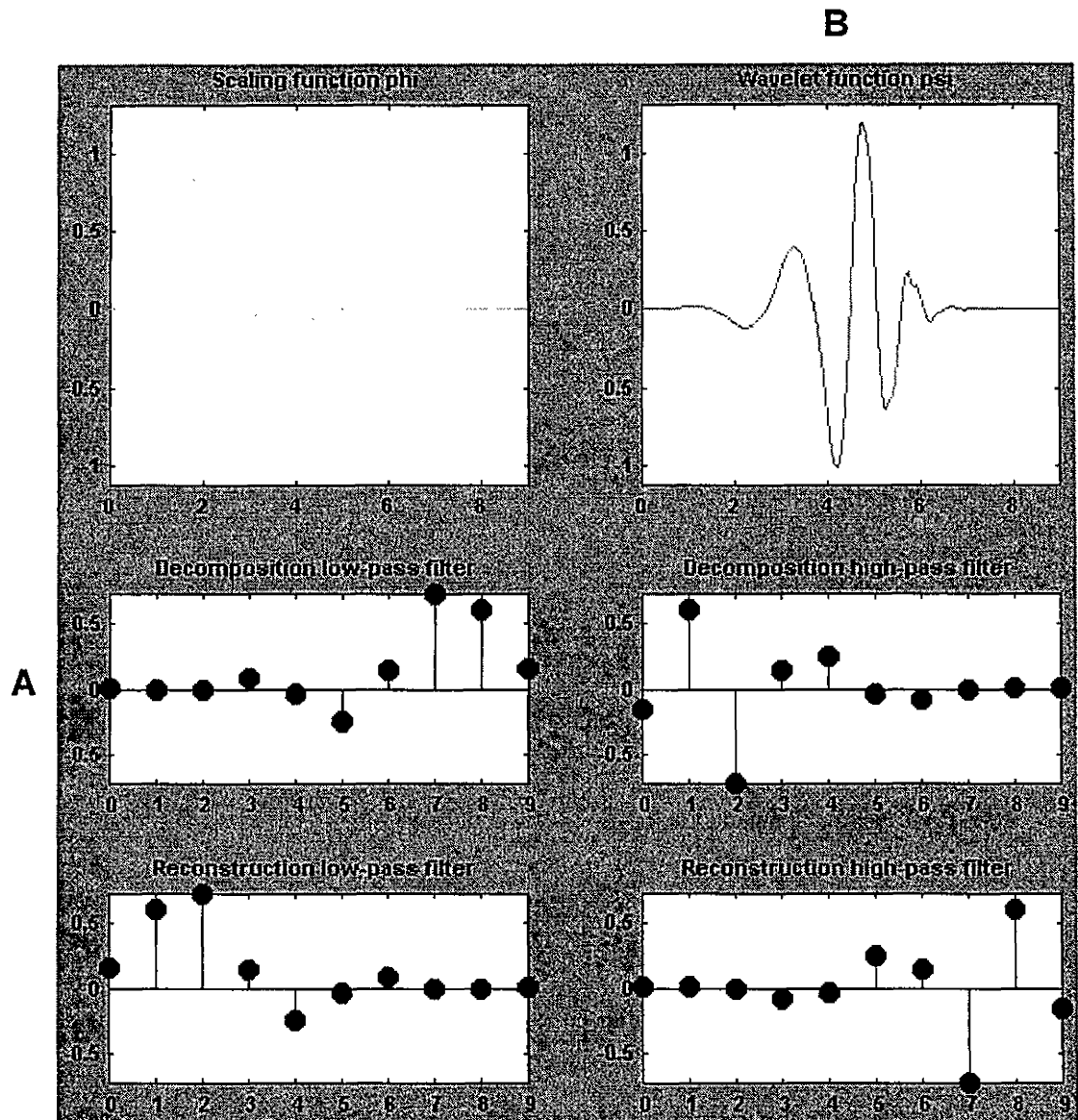


Figure 5.1. Daubechies 'db5' Wavelet Function (B) and Filter Representation (A).

fifth order Daubechies 'db5' wavelet basis, whose waveform, shown in Figure 5.1 (B), is similar to the multiphasic EMG signals being studied.

Mathematically, the continuous wavelet transform (CWT), is defined as the sum over all time of the signal multiplied by scaled, shifted versions of the wavelet function ψ :

$$C(\text{scale}, \text{position}) = \int_{-\infty}^{\infty} f(t) \Psi(\text{scale}, \text{position}, t) dt \quad 5.4$$

The result of the CWT is a set of many wavelet coefficients C , which are a function of scale and position. Multiplying each coefficient by the appropriately scaled and shifted wavelet yields the constituent wavelets of the original signal.

Scaling a wavelet simply means stretching (or compressing) it, and is analogous to changing the period of a sinusoid. As with the period of a sinusoid, the scale factor (usually denoted a) is inversely related to the constituent frequency of the signal features represented by the wavelet coefficients. The higher the scale, the more stretched the wavelet, the longer the segment of the signal with which it is being compared, and thus the lower the frequency of signal features represented by the wavelet coefficients. Conversely, the lower the scale, the more compressed the wavelet, the shorter the segment of the signal with which it is being compared, the more rapidly changing the details, and thus the higher the frequency of signal features represented by the wavelet coefficients.

Shifting a wavelet simply means delaying (or accelerating) its onset. In mathematical terms, delaying a wavelet function $\psi(t)$ by k is represented by $\psi(t-k)$.

Calculating wavelet coefficients at every possible scale and position, as may be done with the CWT, is an impractical computational task resulting in a large amount of redundant information. However, if a subset of scales and positions is chosen based on powers of two – called dyadic scales and positions – then the analysis will be much more efficient and just as accurate. The continuous wavelet transform of Equation 5.4 becomes the discrete wavelet transform (DWT):

$$C(b, a) = \frac{1}{\sqrt{a}} \int_{-\infty}^{\infty} f(t) \Psi\left(\frac{t-b}{a}\right) dt \quad 5.5$$

where,

$$a = \frac{1}{2^j}, \quad b = \frac{k}{2^j}, \quad (j, k) \in Z, \quad Z \text{ being the integer set.}$$

The DWT was implemented in an efficient filtering scheme by Mallat (1989). The Mallat algorithm is actually a classical signal processing scheme called a two-channel subband coder using quadrature mirror filters (Strang and Nguyen, 1996). This practical filtering algorithm yields a fast wavelet transform, into which a signal passes, and out of which coefficients emerge.

For most signals, the low frequency content is the most important part, giving the signal its identity, while the high frequency content provides details. For this reason, in wavelet analysis, the low frequency, high scale components of the signal are known as approximations, while the high frequency, low scale components are known as details. The filtering process, at its most basic level, is shown in Figure 5.2.

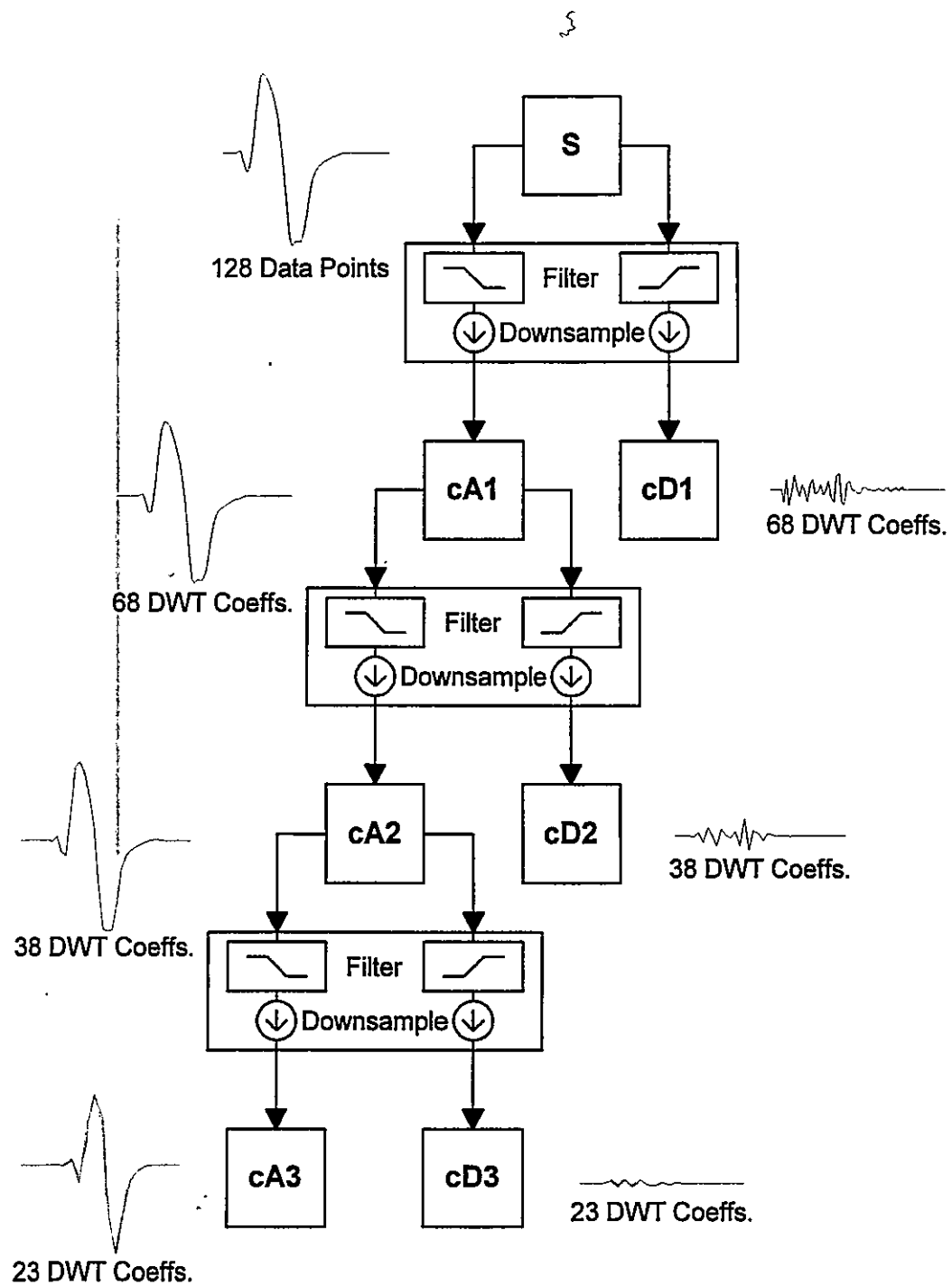



Figure 5.2. Wavelet Decomposition


The signal, S , passes through two complementary filters, one high-pass and one low-pass, emerging as two new signals. Since each of the new signals contains as many samples as the original, downsampling is performed to correct for the doubling in data length. The actual lengths of the resulting detail (cD) and approximation (cA) coefficient vectors are slightly more than half the length of the original signal. This is due to the filtering process, in which the signal is convolved with a filter, introducing several extra samples into the result.

The decomposition process can be iterated, with successive approximations being decomposed in turn, so that one signal is broken down into many lower-resolution components, as shown in Figure 5.2. In theory, this iterative analysis process can be continued indefinitely. In reality, the decomposition can proceed only until the individual details consist of a single sample. In practice, a suitable number of levels is selected based on the nature of the signal, or on a suitable criterion such as entropy. For the purposes of this study, several M-waves were examined using the Matlab 1-D wavelet toolbox. Using the Shannon entropy measure (Coifman and Wickerhauser, 1992), it was determined that the optimum level of decomposition for a typical M-wave with a 'db5' wavelet is 3. At this level of decomposition, minimum-entropy is achieved, and further splitting is not of any interest. The resulting wavelet decomposition of the signal S analyzed at level 3 has the following structure: $[cA_3, cD_3, cD_2, cD_1]$. This array of coefficients, calculated for any two M-waves, can be used to determine the level of similarity (or difference) between them.

5.5 Manual Pattern Recognition

In order to examine the relative efficacy of time, spectral and wavelet features in grouping and differentiating M-waves, an optimal classification scheme must exist. Once all signals are optimally grouped, the inter-group and intra-group separation of time, spectral and wavelet feature sets may be analyzed to reveal which type of features best discriminate responses. Desirable features will minimize an intra-group distance measure between feature vectors, while maximizing the inter-group distance measure. For these studies, the commonly employed Euclidean distance measure was chosen. 

To create a set of optimally classified templates for each of the six studies, spreadsheets were used to manually group and differentiate M-waves. Responses were first sorted by area. With the aid of spreadsheet graphs, the responses were then rearranged manually according to visual inspection, until the first two hundred or so M-waves were grouped into an ideal set of templates. Time constraints and excessive alternation precluded further classification.

Although personal judgement played a key role in determining the optimum classification to which the systems would be compared, similar studies in the past have also used a trained eye as the basis for comparison (Doherty and Brown, 1993; McComas et al., 1971; Stein and Yang, 1990). Since in this case, the goal of EMG pattern recognition is to mimic the decision-making ability of the human brain, it makes sense to use human judgement as the basis of comparison for automated techniques. 

5.6 Feature Comparisons

Six features sets were selected and their relative efficacy for pattern recognition was determined using the manually decomposed signal sets described above. The six feature sets were constructed as follows:

- 1) All time domain response samples (approximately 72 non-zero features).
- 2) Area, peak to peak magnitude and latency of the response.
- 3) Power spectral coefficients (20 past DC). See Section 3.2.4.7.
- 4) All wavelet coefficients (approximately 94 non-zero features).
- 5) Detail wavelet coefficients only (approximately 80 non-zero features).
- 6) Variance of A1, D1, D2 and D3 wavelet coefficient sets and the difference in variance between levels (7 features in total).

In each case, the Euclidean distance measure outlined in Section 3.2.7 was used to determine intra-group and inter-group distances. Inter-group distance was measured between centers, which were determined by taking the mean feature set for each group. Intra-group distance was determined in two ways. First, by taking the standard deviation of individual group members from the mean, and second, by noting the maximum individual's distance from the mean. Relative efficacy of the feature sets was measured by taking the ratio of inter-group distance to each of the intra-group distance measures.

A good feature set will result in a high ratio, reflecting a relatively large distance between neighbouring groups with tight intra-group dispersion. The first ratio, shown in Table 5.1, using standard deviation of intra-group distance represents an average statistic.

The second ratio, shown in Table 5.2, using maximum intra-group deviation represents a worst case measure. Any feature set with a ratio below unity will likely result in misclassification of some signals, since neighbouring groups will overlap.

Table 5.1. Classification Feature Comparison by Intra-Group Standard Deviation

Minimum Inter-Group Distance / Intra-Group Standard Deviation						
	Time		Frequency		Wavelet	
	Response	Area & Pk	Spectrum	All Coeffs.	Detail Only	Level Var.
1L	2.34	1.59	4.04	2.29	1.88	1.26
1R	2.66	1.80	3.30	3.22	2.64	1.79
2L	2.50	1.70	4.42	2.61	2.14	1.43
2R	1.73	1.17	4.85	1.76	1.45	0.97
3L	2.01	1.37	4.55	2.05	1.68	1.13
3R	1.14	0.78	1.34	1.14	0.94	0.63
All	2.06	1.40	3.75	2.18	1.79	1.20

Table 5.2. Classification Feature Comparison by Maximum Intra-Group Deviation

Minimum Inter-Group Distance / Intra-Group Maximum Deviation						
	Time		Frequency		Wavelet	
	Response	Area & Pk	Spectrum	All Coeffs.	Detail Only	Level Var.
1L	1.50	0.87	2.06	1.46	1.20	0.66
1R	1.85	1.04	2.21	2.24	1.83	0.97
2L	1.88	1.09	3.16	1.96	1.61	0.88
2R	1.16	0.67	3.18	1.18	0.97	0.53
3L	1.32	0.76	2.87	1.34	1.10	0.60
3R	0.77	0.44	0.79	0.76	0.63	0.34
All	1.41	0.81	2.38	1.49	1.22	0.66

It is clear from the ratios shown in the classification feature comparison tables above that the frequency domain spectral coefficients are superior to both the time and wavelet based feature sets. Time response features are a good set, but suffer from latency shifting as described earlier in Section 5.1.1. This weakness in using features based on time or Fourier parameters containing phase information was noted by Cavasin (1989), a realization that prompted his subsequent use of power spectral coefficients, which neglect

both time and phase information. Wavelet coefficients are also a good feature set, but again suffer from small latency shifts affecting the position variables of Equations 5.4 and 5.5. As expected, area & peak amplitude of the time response performed poorly since they are only two parameters describing a complex shape. Similarly, the wavelet coefficient level variance feature set performs poorly at differentiating the complex M-waves. Wavelet detail coefficients, which do not include the level 3 approximation coefficients (cA3), provide a feature set with somewhat poorer performance than that of the full set of wavelet coefficients. In contrast with these findings, recent work on decomposition of MU potential trains by Fang et al. (1999) achieved superior classification of EMG potentials when wavelet coefficients related to low frequency interference were excluded from the feature set. However, the difference in findings may be explained by the difference in application. In the study by Fang et al., the excluded low frequency wavelet coefficients were likely affected by noise due to the varying baseline of MU potential trains from which the M-wave potentials were extracted. The baselines of M-waves in the present study are relatively stable, and low frequency noise is therefore less significant.

5.7 Online vs Offline M-Wave Pattern Recognition

The present M-wave pattern recognition system is an online technique, which classifies responses as they are collected. The operator (or software) can thus determine which stimulation levels need further exploration as the recording session progresses. In contrast, offline techniques such as those presented by Milner-Brown and Brown (1976)

and more recently Slawnych et al. (1996) analyze and classify response sequences only after all of the data has been acquired. To ensure that offline techniques such as these do not miss any CR increments, an exhaustive number of responses must be collected.

While online techniques enjoy great efficiencies over offline techniques, a common criticism of online techniques is their dependence on input order of responses. If the classification features of the first responses collected for each group are not representative of the mean of the entire group, the center of that group will be misplaced from the start, increasing the chances of that group overlapping with its neighbours. Such overlap between neighbouring groups can lead to misclassification of responses. For this reason, the optimal classification schemes for the six thenars discussed in this chapter were determined using offline, visual clustering.

The online response classifications of the present system (see Section 3.2.7) differed only slightly from the optimal classification schemes, with a probability of misclassification of less than 2%. In comparison, the technique presented by Slawnych et al. (1996), which uses time response features to classify responses through offline clustering, demonstrates a misclassification probability of 5%. The success of the present system at correctly classifying online responses may be attributed to its use of power spectral classification features over time responses, which are used by Slawnych et al. (1996). By using superior feature sets such as power spectral coefficients, which maximize inter-group distance and minimize intra-group deviation, the system becomes less susceptible to misclassification of responses for any reason, including input order.

However, the present system may be improved by implementing an online clustering algorithm at various stages of the recording session similar to that proposed by Slawnych et al. (1996). While computationally intensive for an online recording session, such an improvement is possible due to the ever-increasing computing speed available to EMG researchers. Reorganization of the templates at various stages of the recording session could help ensure that group centers are appropriately positioned, and new responses are therefore classified as optimally as possible. Dependence on input order of responses would be minimized, while the efficiency, control, feedback and other desirable characteristics of the present online system would remain intact.

CHAPTER 6 CONCLUSIONS

6.1 Summary

The system developed in the present study has the potential of providing a practical and sensitive means for studying the electrical and contractile properties of human motor units *in vivo*. The instrumentation is easy to apply and the subject experiences no discomfort since the limb is not rigidly constrained. As well, a typical recording session consisting of subject instrumentation, determining maximum and sub-threshold responses and obtaining the results for 10 to 20 motor units takes no more than 30 minutes. The approach is noninvasive and therefore avoids pain and tissue injury.

Results were obtained for the left and right thenars of three healthy male volunteers. For the six thenars, a minimum of 9 and maximum of 17 MUs could be studied, resulting in a total sample of 72 MUs. The electrical properties of the MUAPs sampled, including peak to peak amplitude, area and latency were similar in average and in distribution to those found by other researchers. The units sampled were not obviously biased in favour of units that produced large or small MUAPs or accelerations. Data from individual subjects included units producing both small and large MUAPs and accelerations, with latencies and contractile rates virtually spanning the range of the total population. There was no obvious relationship between magnitude and angle of acceleration. Nor was there any grouping of acceleration vectors, as would indicate that units were sampled from separate muscles within the thenar group.

Absolute values of peak acceleration or latency of peak cannot be directly compared to twitch properties measured in other studies. However, even for the small number of subjects studied, histograms for peak acceleration, peak latency and direction of resultant acceleration vector are similar to those found for peak force, contraction time and direction of resultant force vector in similar MU twitch force studies.

Correlation between peak acceleration and MUAP parameters are similar to correlations between twitch force and MUAP parameters found by other researchers. No significant correlation was found between peak acceleration latency and magnitude of acceleration, a finding consistent with recent human studies. It would therefore seem that the common classification of MUs into slow and fast twitch types as done in other species may prove to be more difficult with human thenar MUs.

In light of the agreement of the present results with similar research using force measurement, it may be concluded that acceleration measurement can be used as an alternative to isometric twitch force measurement and may be more suitable because of the relative ease of instrumentation and lack of subject discomfort. It also follows that a pattern recognition scheme based on MUAPs allows the measurement of contractile properties of many more MUs for each muscle studied than can be accomplished by other published techniques.

Initial comparison of wavelet versus time amplitude and Fourier power spectral features shows that wavelet decomposition of M-waves offers no better results than time templates and worse results than power spectral coefficients due to the inherent position dependent nature of time and wavelet features.

6.2 Future Work

The main problems encountered in data collection have been minimizing the background noise in the acceleration signals and getting the subject to relax. A more robust system for supporting the limb that reduces the effects of room and equipment vibration while maximizing subject comfort would be of some benefit. The effects of lightly restraining the arm and hand with devices such as small sandbags to reduce extraneous movement should also be examined.

Further studies to minimize the uncertainty caused by the alternation phenomenon would be useful. Although the possibility of alternation will always exist when using the McComas technique these uncertainties may be quantified and minimized in future work on alternation detection strategies.

Further investigation into M-wave pattern recognition using wavelet analysis while incorporating the removal of time and latency shifts is warranted. The possibility of modifying the wavelet analysis to make the coefficients less position dependent should be investigated. The present system may also be improved by implementing an online clustering algorithm at various stages of the recording session to minimize the dependence of classification accuracy on input order of responses.

Applied longitudinally, the present system may provide a means of tracking the functional status of representative samples of MU populations in health and disease, and in monitoring their response to interventions. It may serve as a useful supplement to established methods for assessing the natural histories of various motoneuronal diseases

and their responses to treatment. It may also be used to study the effects of training and fatigue on individual MUs, or the effects of aging on the MU population.

REFERENCES

- Ballantyne JP, Hansen S. "A new method for the estimation of the number of motor units in a muscle. 1. Control subjects and patients with myasthenia gravis," *Journal of Neurology, Neurosurgery, and Psychiatry*, 37:907-915, 1974.
- Ballantyne JP, Hansen S. "Computer method for the analysis of evoked motor unit potentials. 2. Duchenne, limb-girdle, facioscapulohumeral and myotonic muscular dystrophy," *Journal of Neurology, Neurosurgery, and Psychiatry*, 38:417-428, 1975.
- Bergmans J. The Physiology of Single Human Nerve Fibres, PhD Thesis. Vander: University of Louvain, 1970.
- Brown WF, Strong MJ, Snow RS. "Methods for estimating numbers of motor units in biceps-brachialis muscles and losses of motor units with aging," *Muscle & Nerve*, 11:423-432, 1988.
- Burke RE, Rudomin P, Zajac FE III. "Catch property in single mammalian motor units," *Science*, 168:122-124, 1970.
- Cavasin R. An Automated Muscle Motor Unit Counting System, Master's Thesis. Hamilton: McMaster University, 1989.
- Chan KM, Doherty TJ, Andres LP, Porter MM, Brown T, Brown WF. "Longitudinal study of the contractile and electrical properties of single human thenar motor units," *Muscle & Nerve*, 21:839-849, 1998.
- Coifman RR, Wickerhauser MV. "Entropy-based algorithms for best basis selection," *IEEE Transactions on Information Theory*, 38:713-718, 1992.
- Daubechies I. "Ten lectures on wavelets," in CBMS-NSF Conference Series in Applied Mathematics, Philadelphia: SIAM, 1992.
- Desmedt JE, Hainaut K. "Kinetics of myofilament activation in potentiated contraction: staircase phenomenon in human skeletal muscle," *Nature*, 217:529-532, 1968.
- Doherty TJ, Brown WF. "The estimated numbers and relative sizes of thenar motor units as selected by multiple point stimulation in young and older adults," *Muscle & Nerve*, 16:355-366, 1993.
- Doherty TJ, Brown WF. "A method for the longitudinal study of human thenar motor units," *Muscle & Nerve*, 17:1029-1036, 1994.

- Doherty TJ, Brown WF. "Age related changes in human thenar motor unit twitch contractile properties," *Journal of Applied Physiology*, 82:93-101, 1997.
- Doherty TJ, Stashuk DW, Brown WF. "Determinants of mean motor unit size: impact on estimates of motor unit number," *Muscle & Nerve*, 16:1326-1331, 1993.
- Duda R, Hart P. Pattern Classification and Scene Analysis, New York: Wiley, 1973.
- Eleveld D. Motor Unit Estimates Through Accelerometry, Master's Thesis. Hamilton: McMaster University, 1992.
- Entran Devices Inc. Accelerometer Specifications and Selection Guide, Fairfield: Entran Devices Inc., 1999.
- Fang J, Agarwal GC, Shahani T. "Decomposition of multiunit electromyographic signals," *IEEE Transactions on Biomedical Engineering*, 46:685-697, 1999.
- Feinstein B, Lindegard B, Nyman E, Wohlfart G. "Morphologic studies of motor units in normal human muscles," *Acta Anatomica*, 23:127-142, 1955.
- Gabor D, "Theory of communication," *Journal of the Institute of Electrical Engineering*, 93:429-457, 1946.
- Galea V, deBruin H, Cavasin R, McComas AJ. "The numbers and relative sizes of motor units estimated by computer," *Muscle & Nerve*, 14:1123-1130, 1991.
- Goswami JC, Chan AK. Fundamentals of Wavelets: Theory, Algorithms and Applications, New York: Wiley, 1999.
- Gravel D, Belanger AY, Richards CL. "Study of human muscle contraction using electrically evoked twitch responses during passive shortening and lengthening movements," *European Journal of Applied Physiology and Occupational Physiology*, 56:623-627, 1987.
- Guyton AC, Hall JE. Textbook of Medical Physiology, New York: W.B. Saunders Co., 1996.
- Henneman E, Mendell LM. "Functional organization of the motoneurone pool and its outputs," In Handbook of Physiology, Brooks VB (ed.), Bethesda: American Physiology Society, 1981.
- Isley MR, Krauss GL, Levin KH, Litt B, Shields RW, Wilbourn AJ. Electromyography/ Electroencephalography, Redmond: SpaceLabs Medical Inc., 1993.

- Jasechko JG. Automatic Estimation of the Number of Muscle Motor Units, Master's Thesis. Hamilton: McMaster University, 1987.
- Mallat S. "A theory for multiresolution signal decomposition: the wavelet representation," *IEEE Pattern Analysis and Machine Intelligence*, 11:674-693, 1989.
- McComas AJ. "Motor unit estimation: anxieties and achievements," *Muscle & Nerve*, 18:369-379, 1995.
- McComas AJ, Fawcett PRW, Campbell MJ, and Sica REP. "Electrophysiological estimation of the number of motor units within a human muscle," *Journal of Neurology, Neurosurgery and Psychiatry*, 34:121-131, 1971.
- McComas AJ, Galea V, deBruin H. "Motor unit populations in healthy and diseased muscles," *Physical Therapy*, 73:868-877, 1993.
- Milner-Brown HS, Brown WF. "New methods of estimating the number of motor units in a muscle," *Journal of Neurology, Neurosurgery and Psychiatry*, 39:258-265, 1976.
- Milner-Brown HS, Stein RB, Yemm R. "The contractile properties of human motor units during isometric voluntary contractions," *Journal of Physiology*, 228:285-306, 1973.
- Misiti M, Misiti Y, Oppenheim G, Poggi JM. Wavelet Toolbox User's Guide, Natick: The MathWorks, Inc., 1996.
- National Instruments Inc. Labview User Guide, Austin: National Instruments Inc., 1998.
- National Instruments Inc. PCI-6024E User Manual, Austin: National Instruments Inc., 1998.
- Proakis JG, Manolakis DG. Digital Signal Processing: Principals, Algorithms and Applications, New York: Prentice Hall, 1995.
- Rafuse VF, Gordon T. "Self-reinnervated cat medial gastrocnemius muscles. II. Analysis of the mechanisms and significance of fibre type-grouping in reinnervated muscles," *Journal of Neurophysiology*, 75:282-297, 1996.
- Rafuse VF, Pattullo MC, Gordon T. "Innervation ratio and motor unit force in large muscles: a study of chronically stimulated cat medial gastrocnemius," *Journal of Physiology*, 499:809-823, 1997.
- Sica REP, McComas AJ. "Fast and slow twitch units in human muscle," *Journal of Neurology Neurosurgery and Psychiatry*, 34:113-120, 1971.

- Sica REP, McComas AJ, Upton ARM, Longmire D. "Motor unit estimation in small muscles of the hand," *Journal of Neurology, Neurosurgery and Psychiatry*, 37:55-67, 1974.
- Slawnych M, Laszlo C, Hershler C. "Motor unit estimates obtained using the new MUESA method," *Muscle & Nerve*, 19:626-636, 1996.
- Stashuk DS, deBruin H. "Automatic decomposition of selective needle detected myoelectric signals," *IEEE Transactions on Biomedical Engineering*, 35:1-10, 1988.
- Stein RB, French AS, Mannard A, Yemm R. "New methods for analysing motor function in man and animals," *Brain Research*, 40:187-192, 1972.
- Stein RB, Yang JF. "Methods for estimating the number of motor units in human muscles," *Annals of Neurology*, 28:487-495, 1990.
- Stephens JA, Usherwood TP. "The mechanical properties of human motor units with special reference to their fatiguability and recruitment threshold," *Brain Research*, 25:91-97, 1977.
- Strang G, Nguyen T. Wavelets and Filter Banks, New York: Wellesley-Cambridge Press, 1996.
- Sun M, Sclabassi RJ. "Wavelet feature extraction from neurophysiological signals," In Time Frequency and Wavelets in Biomedical Signal Processing, Akay M (ed.), New York: IEEE Press, 305-321, 1997.
- Szlavik R, deBruin H. "The effect of stimulus current pulse width on nerve fiber size recruitment patterns," *Medical Engineering & Physics*, 21:507-515, 1999.
- Taylor A, Stephens JA. "Study of human motor unit contractions by controlled intramuscular microstimulation," *Brain Research*, 117:331-335, 1976.
- Thomas CK, Johansson RS, Bigland-Ritchie B. "Attempts to physiologically classify human thenar motor units," *Journal of Neurophysiology*, 65:1501-1508, 1991.
- Thomas CK, Johansson RS, Westling G, Bigland-Ritchie B. "Twitch properties of human thenar motor units measured in response to intraneural axon stimulation," *Journal of Neurophysiology*, 64:1339-1346, 1990.
- Westling G, Johansson RS, Thomas CK, Bigland-Ritchie B. "Measurement of contractile and electrical properties of single human thenar motor units in response to intraneural motor-axon stimulation", *Journal of Neurophysiology*, 64:1331-1338, 1990.